A MINIATURE FLAME FOR ATOMIZATION IN CONTINUUM EXCITED ATOMIC FLUORESCENCE SPECTROMETRY

Steven Kenneth Hughes

1979

A MINIATURE FLAME FOR ATOMIZATION IN CONTINUUM EXCITED ATOMIC FLUORESCENCE SPECTROMETRY

by

STEVEN KENNETH HUGHES

B.S., Arizona State University, 1977

A MASTER'S THESIS

submitted in partial fulfillment of the

requirements for the degree

MASTER OF SCIENCE

Department of Chemistry

KANSAS STATE UNIVERSITY
Manhattan, Kansas

1979

Approved by:

Robert C. Fry
Major Professor

Acknowledgment

I would like to thank my wife, Louise, my children, and my parents, Elmo I. and Mildred S. Hughes for the help, understanding and encouragement they gave to me as I pursued this degree. My deepest thanks to Dr. R. C. Fry for his help, guidance and friendship while at Kansas State University.

I thank Dr. C. E. Meloan and Dr. M. van Swaay for their help and a special thanks to Robert Brown for his help. My thanks to Dr. W. G. Fateley, the faculty and staff of the Chemistry Department. For help in building and maintaining my equipment I thank Mr. Al Nielson, Mr. Al Weyerts and Mr. M. Ohno.

TABLE OF CONTENTS

LIST OF FIGURES

LIST OF TABLES

Chapter 1

Introduction

Wood (1905) first observed the phenomenon of resonance atomic fluorescence in sodium vapor. Nineteen years later, Nichols and Howes (1924) reported the atomic fluorescence of Ba, Ca, Li, Na, and Sr in flames. Then Badger (1929) observed the atomic fluorescence of Ag, Cd, Cu, Mg, Na and Tl in flames. Research efforts in this area were renewed by Winefordner and Vickers (1964) and Winefordner and Staab (1964A, 1964B). The new emphasis was on analytical applications of atomic fluorescence.

These analytical studies involved the use of low temperature, low background emission, hydrogen supported flames and the use of low intensity hollow cathode and metal vapor discharge lamps. Both turbulent and laminar flow burners were employed. For many elements and sample matrices the results were characterized by low atomization efficiency. For atomic fluorescence, the signal (I_F) is proportional to both the free atom concentration (C) and the relative intensity of the excitation source (I_o):

$$I_F = k\, I_o\, C$$

All of these systems led to poor detection limits and severe interferences caused by scattered light and incomplete compound vaporization. With the advent of highly efficient atomization techniques (premixed hydrocarbon flame systems) the interferences were brought under control. The addition of high intensity monochromatic excitation sources (microwave excited continuous wave

electrodeless discharge lamps (EDL) and tunable dye lasers) resulted in a "single-element-per-trial" analytical fluorescence method that compared favorably with existing atomic emission or flame atomic absorption spectrometry in detection limits, reproducibility, and tolerance of complex digested sample matrices.

In an effort to develop an atomic fluorescence technique for rapid multi-elemental analysis, Veillon, Parsons, Mansfield, and Winefordner (1964) initiated the use of continuum source (150-w Xenon Lamp) excitation. To improve this technique, a twofold problem had to be solved. Foremost, the relatively low continuum source intensity (I_o) integrated over a wavelength interval equivalent to that of the atomic absorption line width ($\sim$ 0.001 nm) results in poor sensitivity and detection limits ($I_F = kI_oC$). Next, undesired scattered radiation due to incompletely vaporized droplets, salts, etc. is integrated over a wavelength interval equivalent to the instrument bandpass ($\sim$ 0.4 nm) when a continuum excitation source is employed. Consequently, high background interference and immense noise are present.

High temperature premixed hydrocarbon flames have helped reduce the magnitude of scattered light signals (Johnson, Plankey, and Winefordner (1975)). In an effort to increase the source intensity and improve the detection limits Johnson, Plankey, and Winefordner (1974) used a Varian EIMAC xenon short arc continuum source. This source has an unusually high collection efficiency of $\sim$ 90%, a narrow 0.9 mm arc gap, and a 150-500 w power dissipation. The spectral output of the EIMAC lamp measured over a wavelength interval similar

to that of an atomic line width is greater than or equal to that of hollow cathode lamps (O'Haver, Harnly, and Zander (1978)). EDL and laser excitation sources still remain more intense, but their monochromatic nature precludes any reasonable multi-elemental analysis schemes. Advantages of the EIMAC source include the determination of many elements with one source and the simple nature of atomic fluorescence (relatively few resonance lines). The single atomic fluorescence source allows easy operation and maintenance, in contrast to atomic absorption where a large number of sources are necessary. The simple resonance atomic fluorescence spectra allow the use of small, inexpensive monochromators of low resolution but large aperature, in contrast to emission spectroscopy which needs high resolution monochromators.

The combination of these features with computer control of the monochromator has made continuum excited atomic fluorescence a potentially useful multi-elemental analytical system (Johnson, Plankey and Winefordner (1975)). Further sensitivity improvements are needed before the part per billion range can be considered routinely accessible.

The investigations described in the present thesis represent an attempt to further increase the analytical sensitivity of this method via improvements in the method of sample introduction and atomization. In all atomic spectral techniques, the sensitivity is directly proportional to the concentration of the analyte in the viewing region. This concentration depends upon the starting sample concentration, the dimensional and dynamic characteristics of the sample introduction technique, and the overall atomization efficiency. Atomization cells can be divided into several categories; flames,

flame heated devices (boats, cups), plasmas and other electrical discharges, chemical volatilization reactions (e.g, covalent hydride and cold vapor Hg reductions), and electrothermal atomizers.

In flame atomization the sample liquid is usually introduced into the flame by aerosol generation. As the sample is exposed to the flame temperature and flame reactions the analyte is converted to the atomic vapor state (Mann, Vickers, and Gulick (1974)). Many analyses today are performed with premixed air-acetylene and nitrous oxide-acetylene flames.

Of the remaining sample introduction techniques only electrothermal atomization will be considered here since the other techniques are either very specialized or do not lend themselves readily to atomic fluorescence spectrometry. Electrothermal atomization is widely used in atomic absorption spectrometry for a variety of samples. Fuller (1977) has reviewed the atomization processes occurring in electrothermal systems. The most common type in use is a graphite furnace or carbon rod design.

Although atomic fluorescence spectrometry has received relatively little attention in comparison to atomic absorption, the atomization principles involved are similar. The purpose of this research is to pave the way for the development of an atomic fluorescence system utilizing a continuum source, an electrothermal atomizer and a small laminar diffusion flame that meets the criteria of capability for multi-elemental response, improved sensitivity and low interference susceptibility.

In considering a new atomic fluorescence system using an electro-

thermal atomizer and miniature flame combination, two questions must be asked. First, what improvement will be made with this system in place of conventional flame systems. Second, could these improvements have been realized without the use of a flame, i.e. with the electrothermal atomizer alone.

The main problems with conventional flame systems are: low atom concentrations in the viewing cell, high emission background, and combustion mixtures with high burning velocity that lead to safety problems. The low atom concentration is due to poor nebulizer and transport efficiency, large internal dimensions, and high flow rates of combustion gas that dilute the analyte concentration excessively. Safety (burning velocity) considerations often limit the choice of high temperature flames to hydrocarbon mixtures which contain many species (CO, CO_2, N_2, etc.) in the viewing cell that can quench the fluorescence of excited states. In addition excessive background emissions of hydrocarbon flames often lead to poor detection limits. Therefore, improvement by virtue of higher atom concentration and a better choice of flame was the goal of the present research.

In response to the second question initial studies performed in this laboratory with a tantalum strip atomizer had such a high non-selective scattering interference signal that the system was pronounced analytically useless. In carbon filament atomic absorption Alger, Anderson, Haines, and West (1971) showed that severe suppression (0-90%) of the selective or analytically important portion of the signal could result from various sample matrices. Atomic absorption (AA)

studies (Fry and Denton 1979) have also indicated that flames are far more suited to the avoidance of molecular spectral interference than isolated electrothermal atomizers. Winefordner (1978) concludes in a review article that "furnaces with inert atmospheres have complex interactions between sample matrix species and the analyte often causing large errors."

In an effort to overcome the problems of both flame and electrothermal atomization systems, a combination of the two was developed in the present studies. The constraints on the flame systems were as follows. To capitalize on the high atom concentration inherent with electrothermal atomization, the internal dimensions should be minimized and the flame gases must not cause excessive dilution. Several previous workers in emission studies have not taken this sufficiently into account (Grime and Vickers (1976), Runnels and Gibson, (1967), Fricke, Rose, and Caruso (1975), Nixon, Fassel, and Kniseley (1974), and Gunn, Millard and Kirkbright (1978)). The flame must have a relatively low concentration of quenching species and must be nonoxidizing in character. The flame should be low in emission background, and it should not be premixed (otherwise the firing of the electrothermal atomizer would detonate the combustion mixture internally). The flow should be laminar to maintain high stability and low flicker noise. The flame must be sufficiently high in temperature to reduce or eliminate the matrix interferences and light scattering problems commonly associated with furnace atomization.

The constraints in practice mean that the flow rate of the miniature flame should be less than 200 mL/min (conventional flames are $\sim$ 10 L/min) and that the flame temperature should be in excess of 2500°K. To reach these conditions a miniature nitrous oxide-hydrogen laminar diffusion flame was developed as part of this research. Comparisons of flame temperatures, burning velocity and spectral background of the new low flow rate nitrous oxide-hydrogen diffusion flame with conventional (10 L/min) hydrogen-entrained air, premixed air-acetylene and premixed nitrous oxide-hydrogen flames are presented in the following chapter.

Chapter 2

Flames for Atomic Fluorescence Spectrometry

Introduction

Earlier atomic fluorescence work on various flame systems (reviewed by Kirkbright and Sargent (1974)) has led to the following overall conclusions. Hydrogen-entrained air systems have a very low spectral background, but exhibit severe interefences deriving from condensed phase species. These are due to the very low flame temperature. Turbulent oxygen-hydrogen and oxygen-acetylene flames were used by Winefordner and Vickers (1964). These flames are useless for elemental determinations in sample matrices. This is due to the large droplets and resultant poor desolvation and atomization in the turbulent nebulizer-flame combination. The limiting factor for these systems is noise from scattered light produced by water droplets not completely vaporized in the flame. Winefordner and Vickers (1964) suggested that a more efficient means of atomization would improve the detection limits and overall reliability.

In recent work, premixed hydrocarbon supported flames of improved atomization efficiency have been used. These flames eliminate many interferences arising from the sample matrix. Now the limitations are the high emission and fluorescence background of flame constituents (which adds noise), low analyte atom concentrations, and the high concentration of quenching species in the flame.

Several premixed flame systems have been reported. These include nitrous oxide-acetylene, argon separated nitrous oxide-acetylene (Weeks, Haraguchi, and Winefordner (1978)), air-acetylene, argon

separated air-acetylene (Fowler and Winefordner (1977)), oxygen-hydrogen and nitrous oxide-hydrogen (Routh (1979)).

The premixed nitrous oxide-acetylene flame, although high in quenching species and emission background is a very efficient high temperature (2950°K) atomization flame with excellent chemical reducing properties, and a moderate burning velocity. This flame is often used in the determinations of elements that would otherwise form refractory oxides. The premixed oxygen-hydrogen flame is a low background, high temperature flame, but owing to its highly oxidizing properties and extreme burning velocity of 1400 cm/sec (Kirkbright and Sargent (1974)), it is generally avoided except in specialized situations.

Weeks, Haraguchi, and Winefordner (1978) reported the fluorescence background spectra of the premixed air-acetylene and argon-separated air-acetylene flames with a continuum excitation source. These are moderate background flames with moderate atomization efficiencies and fair reducing properties. The argon separated flame yields less noise than the conventional premixed flame. Accompanying this noise reduction was a decrease in temperature of about 200°K (Haraguchi, Smith, Weeks, Johnson, and Winefordner (1977)).

Premixed nitrous oxide-hydrogen flames have a background spectrum of moderate intensity. They have a high atomization efficiency. The reducing properties have not been reported. The burning velocity of this flame is 390 cm/sec. The above premixed flames are generally burned at flow rates well above 2 L/min to keep the rise velocity in excess of the burning velocity so that a stable flame front is

maintained on the burner top. Miniaturization is generally not feasible with a premixed system unless the burner port openings are made extremely small.

The ideal flame for use with atomic fluorescence should meet several requirements. The flame should exhibit a low background and low flicker noise. This improves the detection limit. To analyze a complex sample digest, the flame should provide high temperatures and reducing (or at least nonoxidizing) properties. To facilitate easy operator handling and safety, a low burning velocity is required. The potential for reduction in gas flow rates is desired to maintain high atom concentrations.

The following experimental section includes a description of a miniature nitrous oxide-hydrogen diffusion flame developed in the course of this research project. An evaluation of the new flame is presented in terms of background fluorescence spectra of the flame gas constituents, spectrally measured temperature of the flame, and effective burning velocity. Comparisons are also made with conventional combustion mixtures.

Experimental

Apparatus: A block diagram of the experiment is given in figure 1. The beam from an EIMAC xenon short arc (A) source supplied with D.C. power is interrupted by a mechanical chopper (B) at 83 Hz. The source is focussed into the flame (E) by a one inch diameter lens (D) of two inch focal length manufactured (ESCO) from Suprasil #2 grade optical material. The projected spot is 3 mm in diameter and is located at a variable height above the burner top. Field

Figure 1. Schematic Diagram of Continuum Excited Atomic Fluorescence

(A) EIMAC Continuum Source,

(B) chopper,

(C_1-C_4) field stops,

(D) lens,

(E) Burner/nebulizer,

(F) light trap,

(G) lens,

(H) monochromator,

(I) photomultiplier tube,

(J) lock-in amplifier,

(K) recorder,

(L) high voltage power supply

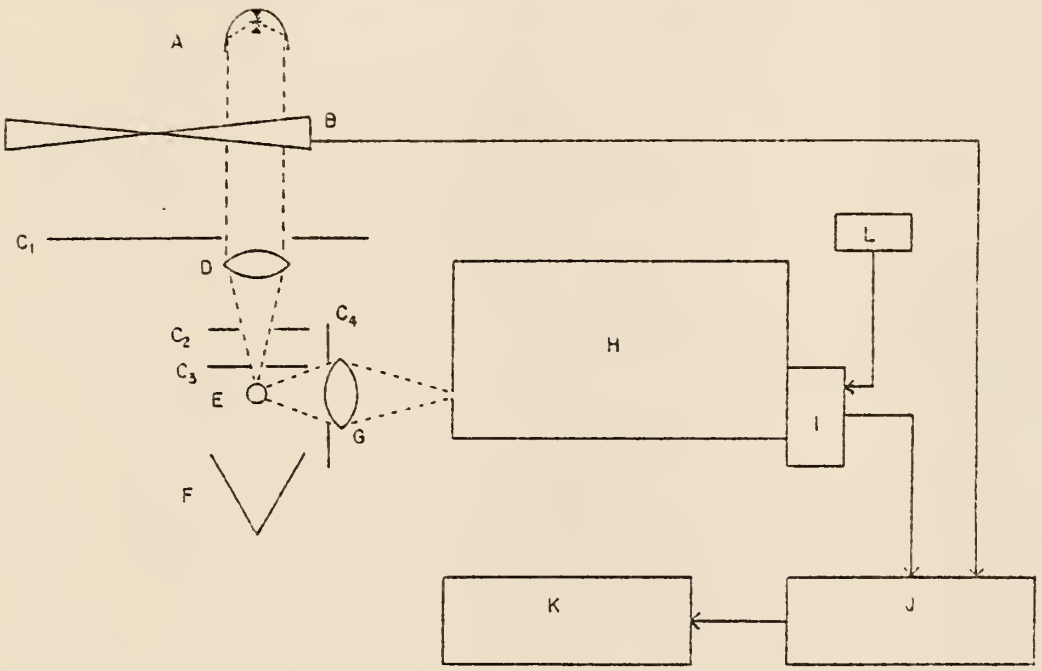
A
B
C1
D
C2
C3
E
C4
G
F
H
I
L
K
J

stops (C_1-C_4) are included to reduce stray light and are of diameters: C_1 - 2.5 cm, C_2 - 1.3 cm, C_3 - .5 cm. C_4 is adjusted so that it fills the solid acceptance angle of the monochromator (H). A light trap (F) is positioned to avoid eye damage and reduce stray light. The fused silica lens combination (G) used to focus the fluorescent radiation onto the monochromator entrance slit is 6 cm in diameter with a combined focal length of 5 cm. The lens is positioned to produce a 4:1 magnification ratio of the flame imaged on the entrance slit. The signal from the photomultiplier (I) is processed with a pre-amp, lock-in amplifier (J), and a frequency reference signal from the chopper (B). The demodulated signal is then recorded on a strip chart recorder (K).

Instrument components used are given in Table I. Experimental conditions are given in Tables II and III.

Combustion Zones in Diffusion Flames

The development of a high temperature miniature oxidant-diffusion flame was desired so that an electrothermal atomizer might be used for sample introduction in the presence of "fuel only". This would avoid rapid oxidation of the atomizer and internal detonation which would otherwise result if the gases were premixed. The diffusion approach also makes it possible to maintain laminar flow.

Development of the high temperature miniature diffusion flame began with studies of hydrocarbon based flames; air-acetylene, oxygen-acetylene, and nitrous oxide-acetylene flames. In all cases the oxidant was allowed to diffuse into the fuel above the burner top. A graphite cup atomizer was located inside the burner head in a

Table I. Experimental Components

Component	Type	Company Address
Monochromator	82-000 focal length - 0.5 m blaze wavelength - 5000 Å ruling density - 30,000 rules/in f/number - f/8.9	Jarrell Ash Waltham, MA 02154
Photomultiplier	R106UH	Hamamatsu Co. Middlesex, NJ 05648
Photomultiplier power supply	82-375-C	Jarrell Ash Waltham, MA 02154
Preamp	A	Princeton Applied Research Princeton, NJ 08540
Lockin	HR-8	Princeton Applied Research Princeton, NJ 08540
Xenon-arc lamp	VIX-300-UV	EIMAC, Div. of Varian San Carlos, CA 94070
Lamp power supply	PS-300-1	EIMAC, Div. of Varian San Carlos, CA 94070
Recorder	355	Linear Instrument Corp. Irvine, CA
Nebulizer	303	Perkin-Elmer Norwalk, CT 06852
Burner	Air/C_2H_2	Unicam (see Figure 3)
Burner	N_2O/H_2 premixed	Laboratory constructed (see Figure 3)
Burner	N_2O/H_2 diffusion	Laboratory constructed (see Figure 3)
Nebulizer	Ultrasonic	Plasma-Therm Inc. Kresson, NJ 08053
Nebulizer power supply	UNPS-1	Plasma-Therm Inc. Kresson, NJ 08053

Table I (continued)

Component	Type	Company Address
Chopper	83Hz	Laboratory constructed
Desolvator		Laboratory constructed
Electrothermal atomizer		Laboratory constructed (see Appendix A)
Power supply - Electrothermal atomizer	Model 61 Carbon Rod Atomizer	Varian Techtron

Table II. Experimental Condition for Fluorescence Studies

Component	Condition
slit width	200 μm
slit height	1.2 cm
band pass	3.37 Å
scan rate	50 Å/min
record rate	2 cm/min
PMT Voltage	780 volts
lamp current (EIMAC source)	20.5 A
time constant	1 sec

Table III. Flame Parameters

Flame (Oxid/Fuel)	Oxid/Fuel (rates L/min)	Observation height (cm)
Background premixed	-/-	2.0
Background diffusion	-/-	0.4
H_2-entrained Air premixed	-/4.0	2.0
H_2-entrained Air diffusion	-/0.16	4.0
Air/C_2H_2 lean	5.5/1.25	2.0
Air/C_2H_2 rich	5.5/1.6	2.0
N_2O/H_2 premixed	3.8/3.5	1.6
N_2O/H_2 diffusion	1.2/0.16	0.4

fuel environment. Each of these diffusion flames exhibited intense incandescence at the fuel-oxidant interface. This was due to insufficient mixing resulting in incomplete combustion of the hydrocarbon fuel. The intense incandescence of incompletely burned carbon particles produced from the fuel rendered these flames useless for analytical purposes. The turning point in this project occurred when we realized that a miniature nitrous oxide-hydrogen diffusion flame could be burned that would not yield incandescence, and would furthermore maintain a desirably high temperature in comparison to relatively cool entrained air-hydrogen flames. To evaluate the relative merit of this diffusion flame a comparison was made with a more conventional premixed nitrous oxide-hydrogen flame.

A premixed nitrous oxide-hydrogen flame contains three major reaction zones or stages (see figure 2A). First a stage that produces no visible emission. The second narrowly confined reaction zone is characterized by a rather intense yellow emission. The third and largest volume reaction zone produces a green emission of relatively low intensity.

In the nitrous oxide-hydrogen diffusion flame developed in the present studies, different conditions exist. This appears to be a fuel rich flame, with only two reaction zones (see figure 2B). The yellow zone found in the premixed flames is missing in the new diffusion flame. Only the colorless and low intensity green regions are present.

It should be noted that the diffusion flame was only successful on a miniature scale (.03-.5 L/min). Attempts to generate normal flame

Figure 2. Optical Profile of Premixed and Diffusion Nitrous Oxide-Hydrogen Flames.

A. Premixed Flame

a) Region of Green Emission
b) Region of No Visible Emission
c) Region of Yellow Emission
f) Premix Gases and Analyte

B. Diffusion Flame

a) Region of Green Emission
b) Region of No Visible Emission
d) N_2O Gas
e) H_2 Gas and Analyte

C. High Flow Diffusion Flame

a) Region of Green Emission
b) Region of No Visible Emission
d) N_2O Gas
e) H_2 Gas and Analyte

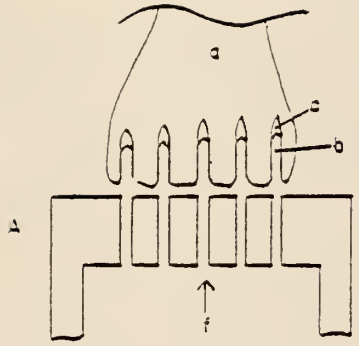
a
c
b
f

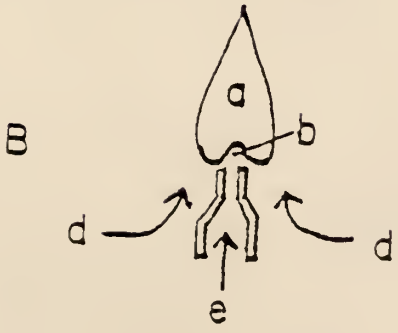
B
a
b
d
d
e

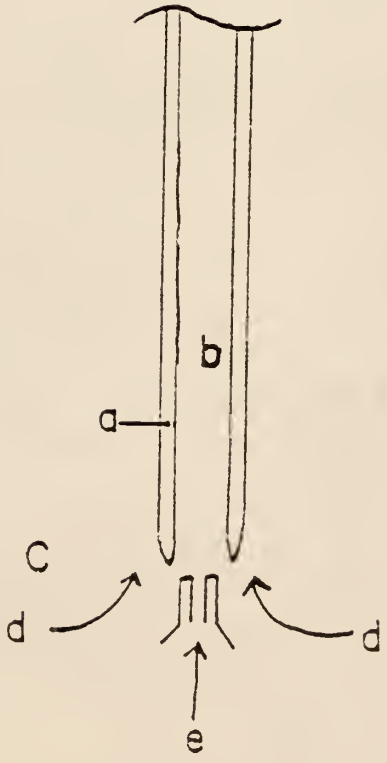
b
a
C
d
d
e

flow rates (8-12 L/min) in a nitrous oxide-hydrogen diffusion flame were unsuccessful. The flame burns only around the perimeter and not in the middle (see figure 2C).

The miniature flame, was however, successful in achieving a useful combustion mantle above the colorless zone, as seen in figure 2B. The following section contains a comparison of background fluorescence of this flame with that of conventional mixtures.

Flame Background Spectra

The instrumental components used in this study were given earlier in Table I. Tables II and III contain the conditions under which the fluorescence background data were taken. The spectrum for each flame was scanned from 200 nm to 600 nm. All flames were operated in their "normal" mode i.e., on the premixed systems, distilled water was aspirated at all times, while in the diffusion system it was not. Portions of the flame spectra have been omitted in figures 1-8. These regions showed no unusual spectral features.

The burner used for all premixed air-acetylene and hydrogen-entrained air studies was a Unicam air-acetylene burner having 13 holes arranged in a square pattern of 1 cm^2 area (see figure 3). The individual hole diameter is 1.25 mm. The nitrous oxide-hydrogen premixed burner was constructed in our laboratory. It has 18 holes arranged in two concentric circles around a central hole (see figure 3). The diameter of the outer circle is 12 mm and the individual hole diameter is 0.9 mm. The burner top is 4.6 mm thick. The diffusion flame is supported on a single hole burner (1.0 mm in diamter) for fuel (H_2) surrounded by a larger concentric opening (6.5 mm in diameter for nitrous oxide (see figure 3).

Figure 3. Burner Design Background Study

A. Premixed Air/C_2H_2 and H_2 entrained air,

a) premixed Gases and Analyte

B. Premixed N_2O/H_2

a) Premixed Gases and Analyte

C. Diffusion N_2O/H_2 and H_2 entrained air

b) H_2 Gas and Analyte

c) N_2O Gas

d) Packing material to promote Laminar Flow

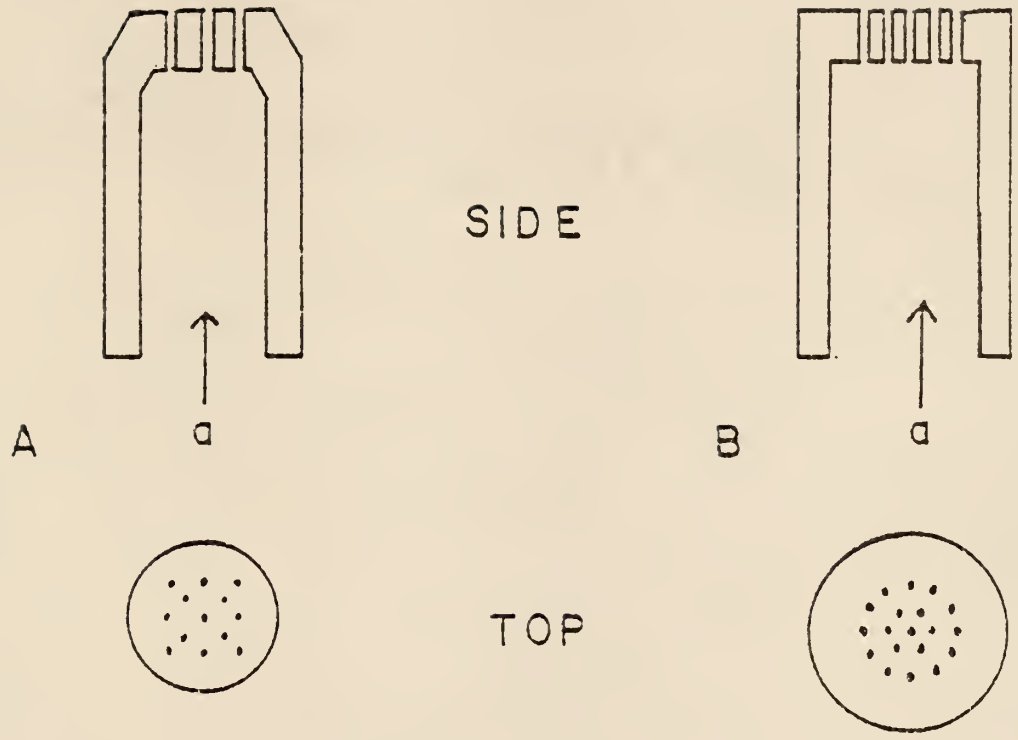
SIDE
A
a
B
a
TOP

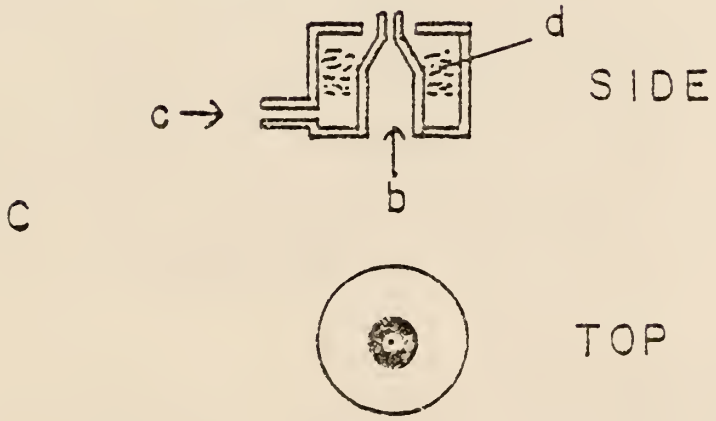
d
SIDE
c
b
C
TOP

The fluorescence spectra of all flames investigated are presented in figures 4-11. The spectra are not corrected for lamp output or detector response. Some stray lamp reflection is still present despite the external field stops and light trap. This is evident in figures 4 and 5 (systems background no flame burning). The features of figure 4 and 5 represent the lamp reflection spectrum (not flame background); they will not be considered in the remaining flame systems. When reviewing figures 6-11, the reader should mentally visualize figure 4 and 5 as the stray reflection baseline. Only spectral features evident in excess of this "baseline" will be attributed to flame gas constituents. The transition assignments for all bands were taken from the work of Fowler and Winefordner (1977) with the exception of the NO band which was taken from Gaydon (1944).

In figure 6 the only additional feature of a conventional argon-hydrogen-entrained air flame burned in a high flow rate spray chamber system is the increase in noise in region A from 280 to 320 nm. This is due to OH emission bands which are rejected in magnitude (the signal is rejected by the lock-in, but not the noise contribution). The OH emission is produced by the $A^2\Sigma$-$X^2\Pi$ transition known as the 306.4 nm system of OH. No net fluorescence of OH is apparent here.

The spectrum of a miniaturized entrained air-hydrogen flame appears in figure 7. We see a fluorescence band in region A. This is also due to the 306.4 nm system of OH. We note that, although it would offset the baseline in an analytical determination, the miniature flame exhibits less noise (figure 7) in the vicinity of 306 nm than does the high flow rate spray chamber-nebulizer (figure 6).

Figure 4. Fluorescence Background - premixed systems - no flame

A. spectral region from 200 nm to 350 nm

B. spectral region from 380 nm to 520 nm

abscissa is in nm

ordinate is relative intensity (arbitrary units)

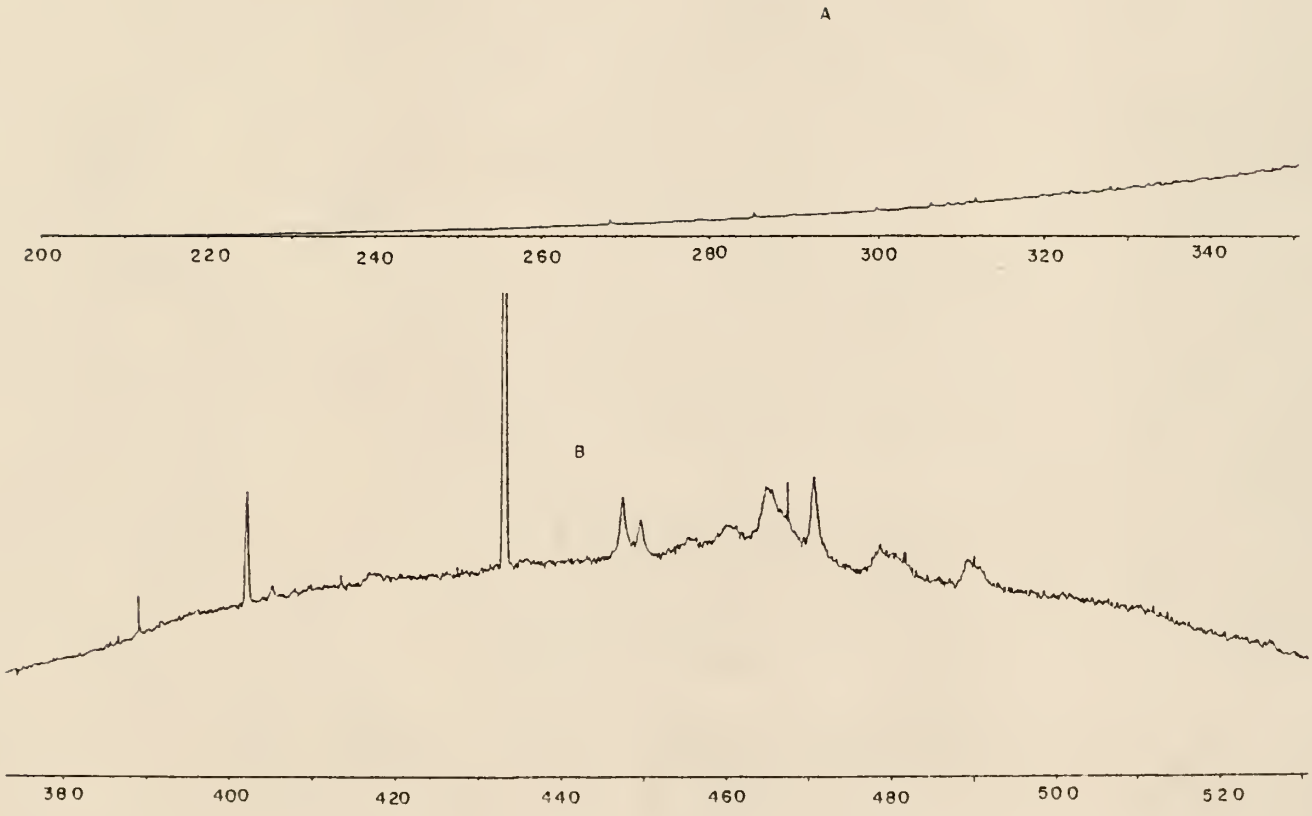
A
200
220
240
260
280
300
320
340
B
380
400
420
440
460
480
500
520

Figure 5. Fluorescence Background - diffusion system - no flame

A. spectral region from 200 nm to 350 nm

B. spectral region from 380 nm to 520 nm

Abscissa is in nm

Ordinate is Relative Intensity (Arbitrary Unit)

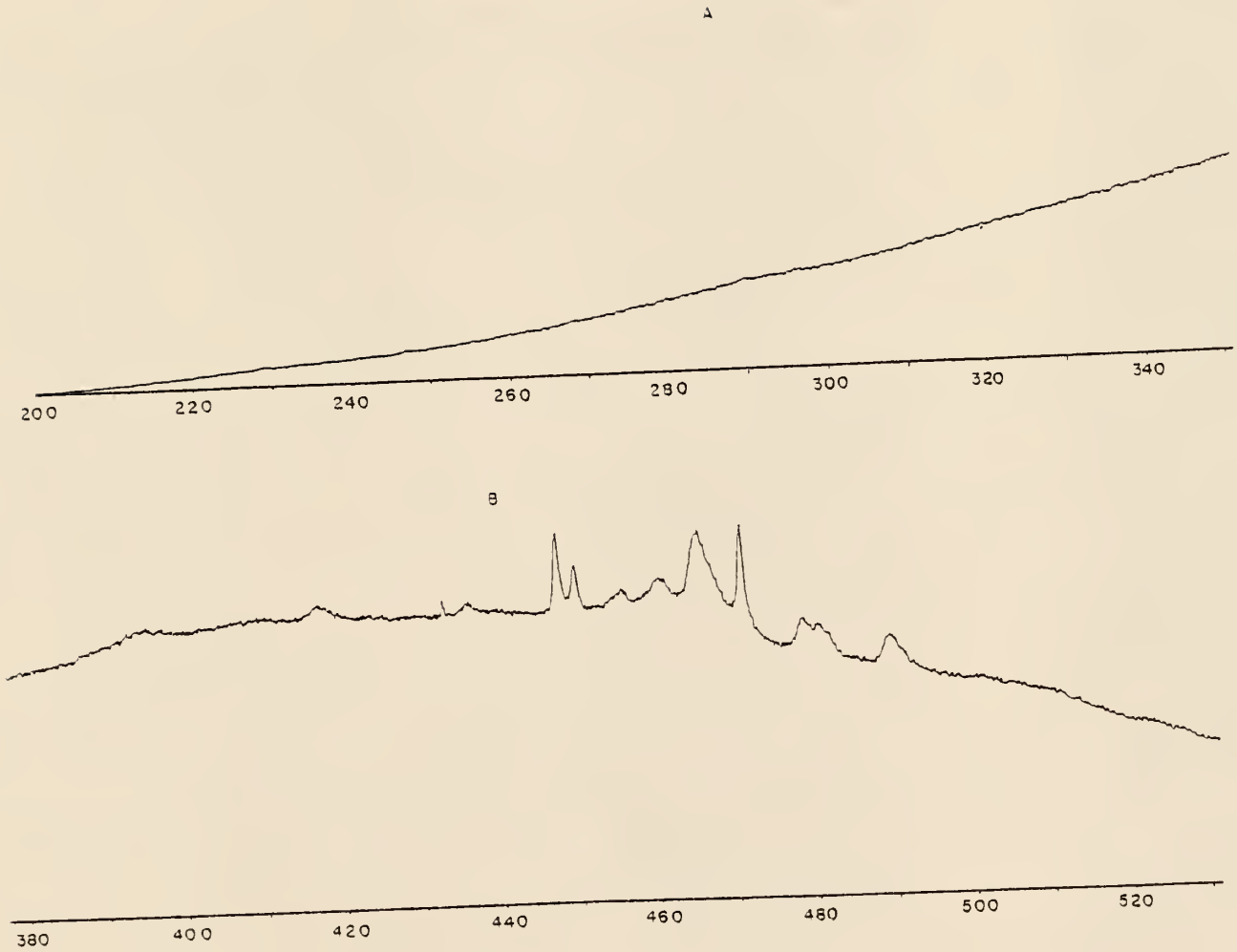
A
200
220
240
260
280
300
320
340
B
380
400
420
440
460
480
500
520

Figure 6. Fluorescence H_2-entrained air, spray chamber system

A. spectral region from 200 nm to 350 nm

B. spectral region from 380 nm to 520 nm

Abscissa is in nm

Ordinate is Relative Intensity (Arbitrary Units)

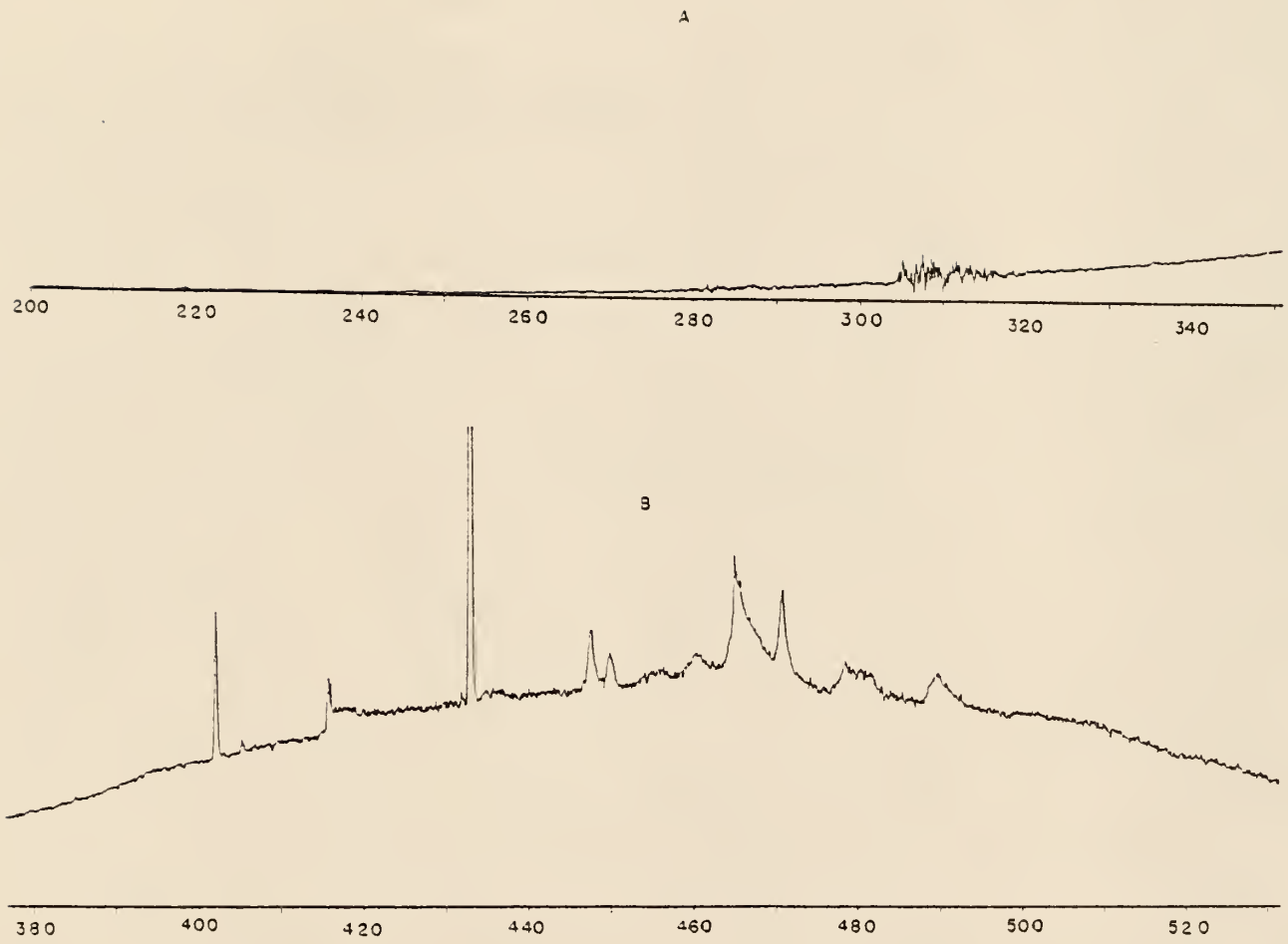
A
200
220
240
260
280
300
320
340
B
380
400
420
440
460
480
500
520

Figure 7. Fluorescence H_2-entrained air, diffusion system

A. spectral region from 200 nm to 350 nm

B. spectral region from 380 nm to 520 nm

Abscissa is in nm

Ordinate is Relative Intensity (Arbitrary Units)

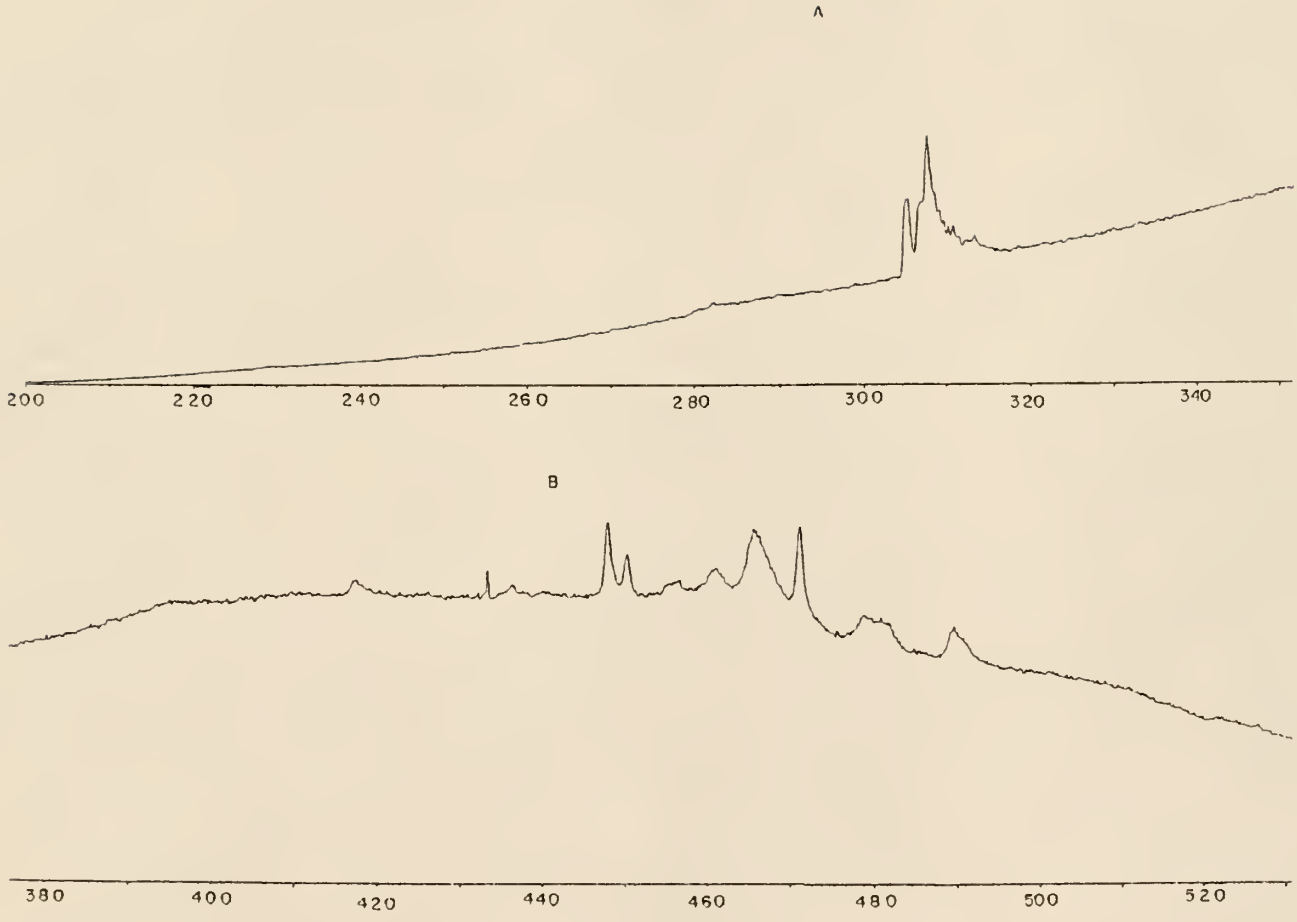
A
200
220
240
260
280
300
320
340
B
380
400
420
440
460
480
500
520

The band fine structure is produced by different vibrational-rotational sublevels associated with the same electronic energy levels.

In figure 8, the fluorescence of a premixed fuel-lean air-acetylene mixture shows a PO fluorescence band between 220 nm and 270 nm. The phosphorus originates from PH_3 contamination in welding grade acetylene. The band arises from the electronic transition $A^2\Sigma-X^2\Pi$ of the γ system of the PO molecule. The 306.4 nm OH band system is also very intense in this mixture.

In figure 9, it is apparent that a fuel-rich premixed air-acetylene flame yields a slight increase in the γ system of the PO molecule. The 306.4 nm fluorescence system of OH is diminished in addition, a band has appeared in region B just above 380 nm that is probably due to the CN violet system, from the $B^2\Sigma-A^2\Pi$ transition of the CN radial. The fluorescence spectrum of a nitrous oxide-hydrogen premixed flame (figure 10) shows fluorescence involving the 306.4 system of OH. There is no observable fluorescence from the PO-γ-system or from the CN violet system. However, in region A from 200 nm to 270 nm additional fluorescence band structure is present. These bands are due to the γ system of NO, the transition to the ground state $X^2\Pi$ from the lowest excited state $A^2\Sigma^+$. The fine structure is due to vibrational-rotational sublevels.

In the nitrous oxide-hydrogen miniature diffusion flame (figure 11), the presence of the 306.4 nm system of OH is noted (with a very low noise contribution). The γ system of NO is increased. But again, there is less noise associated with these bands in the miniature diffusion flame than in the premixed systems.

Figure 8. Fluorescence of a fuel lean air/C_2H_2 premixed flame

A. spectral region from 200 nm to 350 nm

B. spectral region from 380 nm to 520 nm

Abscissa is in nm

Ordinate is Relative Intensity (Arbitrary Units)

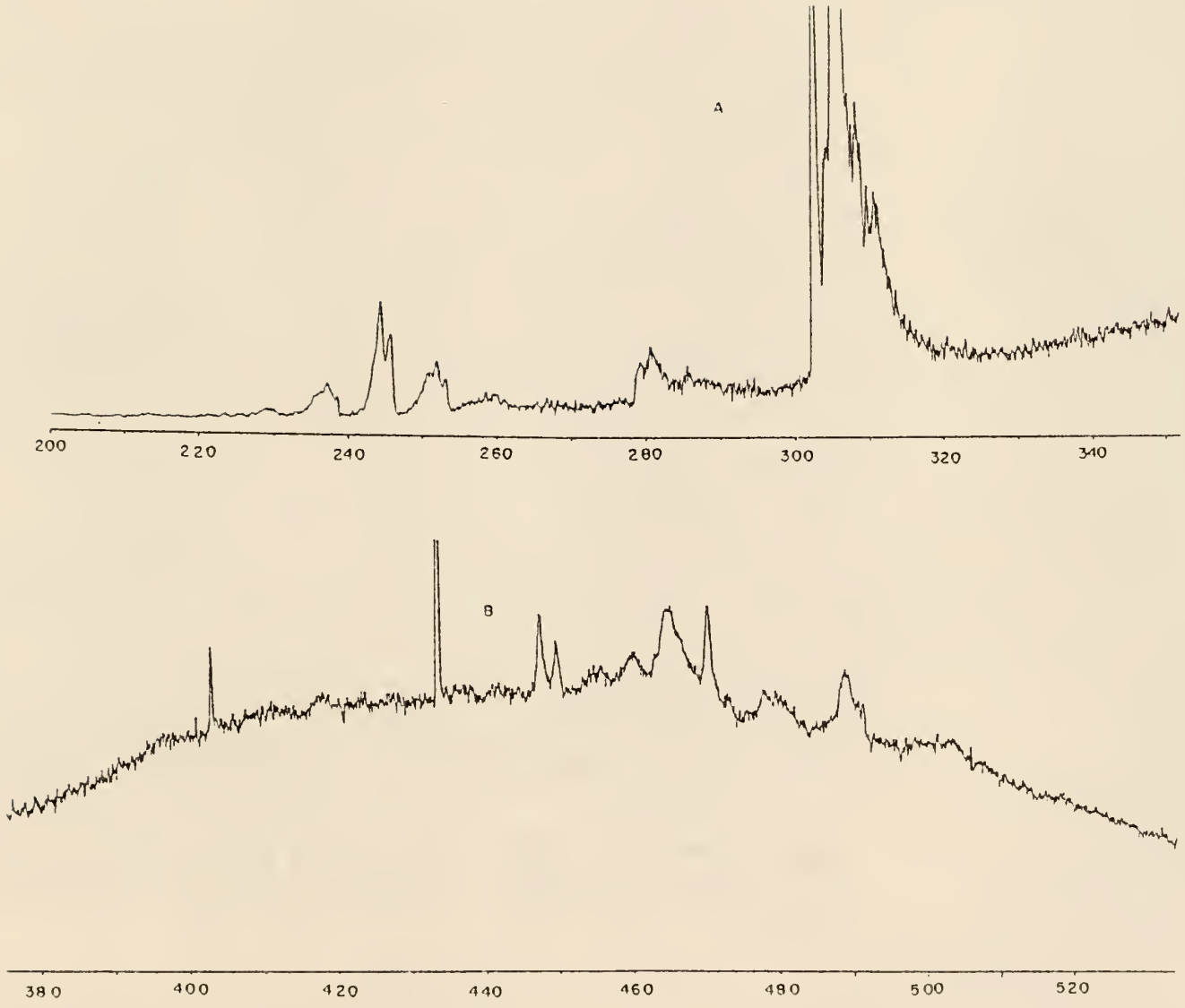
A
200
220
240
260
280
300
320
340
B
380
400
420
440
460
480
500
520

Figure 9. Fluorescence of a fuel rich air/C_2H_2 premixed flame

A. spectral region from 200 nm to 350 nm

B. spectral region from 380 nm to 520 nm

Abscissa is in nm

Ordinate is Relative Intensity (Arbitrary Units)

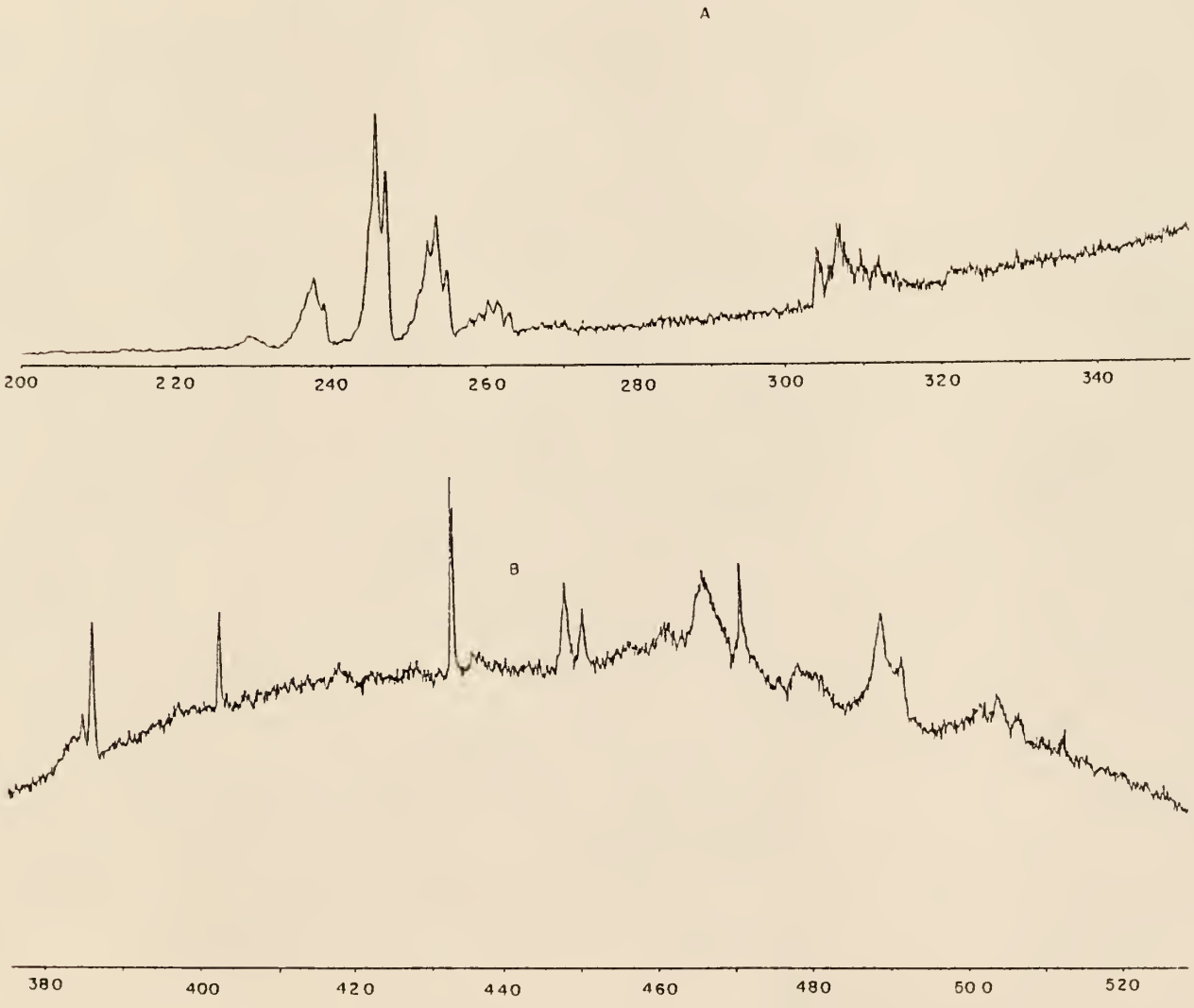
A
200
220
240
260
280
300
320
340
B
380
400
420
440
460
480
500
520

Figure 10. Fluorescence Background N_2O/H_2 premixed flame

A. spectral region from 200 nm to 350 nm

B. spectral region from 380 nm to 520 nm

Abscissa is in nm

Ordinate is Relative Intenstiy (Arbitrary Units)

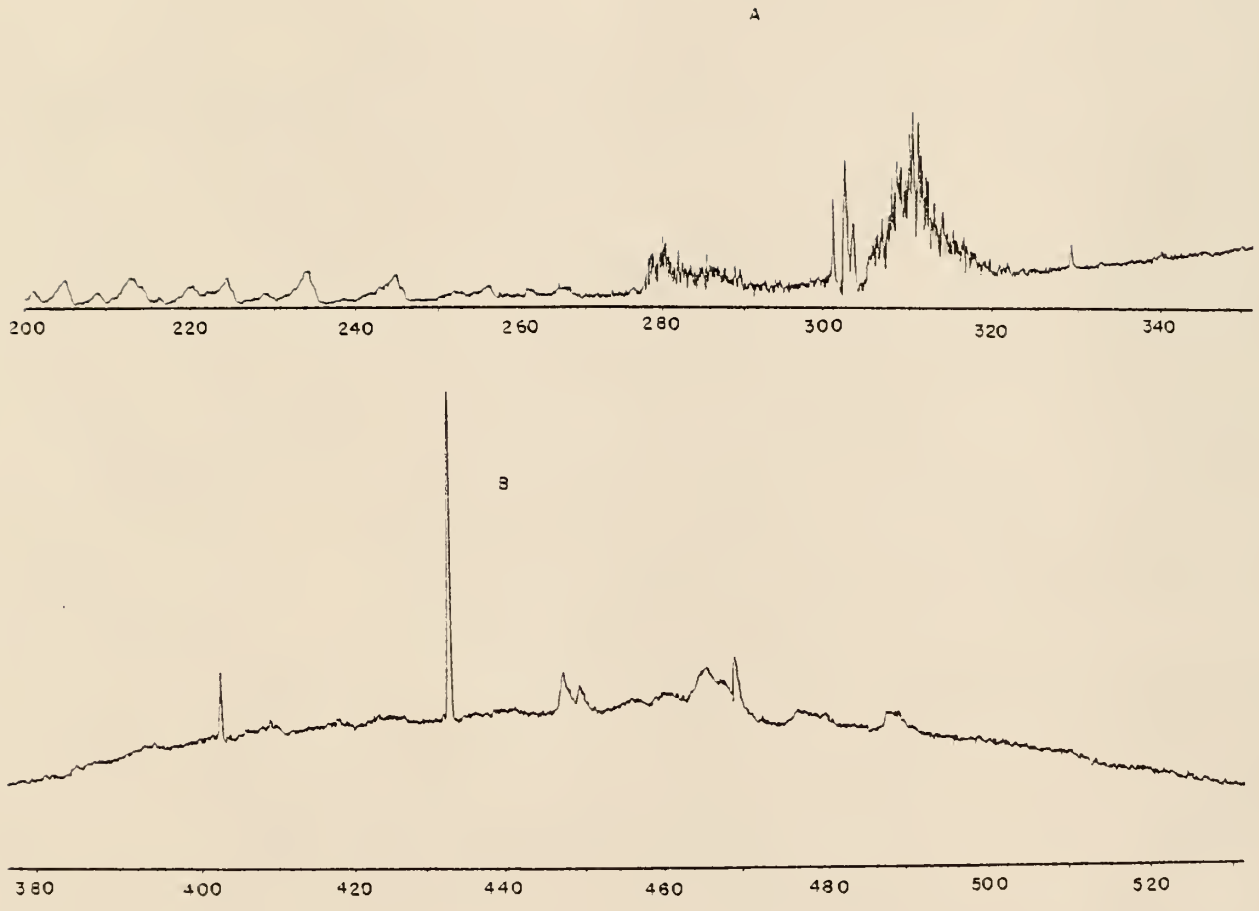
A
200
220
240
260
280
300
320
340
B
380
400
420
440
460
480
500
520

Figure 11. Fluorescence Background N_2O/H_2 diffusion flame

A. spectral region from 200 nm to 350 nm

B. spectral region from 380 nm to 520 nm

Abscissa is in nm

Ordinate is Relative Intensity (Arbitrary Units)

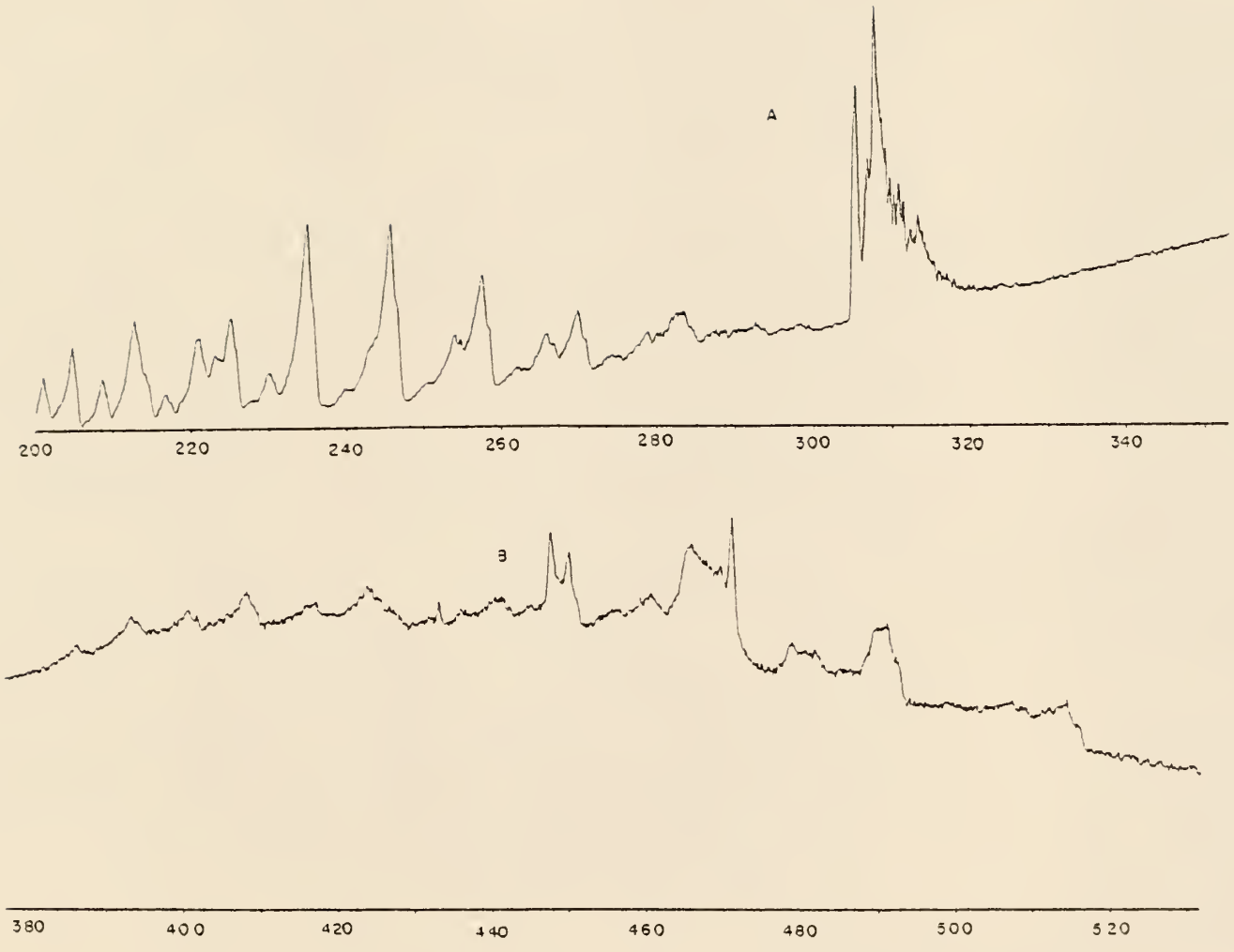
A
200
220
240
260
280
300
320
340
B
380
400
420
440
460
480
500
520

In comparison of wavelength-static measurements of resonance AF line intensities from the diffusion flame and a premixed flame we see that the diffusion flame may require more offset, but there is less overall noise than in the premixed flame.

Temperature Measurement

The flame temperatures reported in this study were obtained from a plot of ln $(gf/\lambda^3 I)$ versus E (3 line emission slope method, Reif, Fassel, and Kniseley (1972)). Here gf is the product of the degeneracy of the excited state and the oscillator strength of the transition, λ is the wavelength, I = relative emission intensity, and E is the energy of the upper level of the electronic transition. The slope is predicted to be 1/kT where k = Boltzmann constant and T = temperature. The slope was calculated by a linear least squares computer routine on a laboratory microcomputer. Physical data involving cobalt lines were obtained from Fernandez and Bastiaans (1979) and are presented in Table IV.

Tables III and V show the conditions for the flame temperature data. The emission spectrum was scanned from 340 nm to 247 nm for cobalt. The cobalt was introduced by nebulizer as a 1000 ppm aqueous standard prepared as outlined by Smith and Parsons (1973).

The relative emission intensity of the cobalt lines in premixed N_2O/H_2 and N_2O/H_2 miniature diffusion flames were measured. (The signal from the flame was modulated by inserting the chopper (B) (see figure 1) between the flame cell (E) and the monochromator (H)). Solution was aspirated with a Perkin-Elmer 303 nebulizer for the premixed system.

Table IV. Properties of the Cobalt Lines Used for Temperature Determinations (from Fernandez and Bastiaans (1979)).

Wavelength (nm)	gf value	Energy(cm^{-1})
340.51	2.7	32842
345.35	4.6	32431
346.58	0.42	28845

Table V. Conditions for Flame Temperature Data

Component	Condition
slit width	20 μm
slit height	1.2 cm
band pass	0.34 Å
scan rate	20 Å/min
record rate	2 cm/min
PMT voltage	780 volts
time constant	1 sec

For the diffusion flame, an ultrasonic nebulizer coupled with a desolvator was used for sample introduction. The desolvator was constructed with 26 gauge nichrome wire wrapped 45 turns about a 18 mm o.d. quartz tube. A concentric heating quartz tube 11 mm o.d. spaced with machinable ceramic washers was placed inside the heated quartz tube and connected through teflon-o-ring connectors to 12/5 glass ball joints to the nebulizer. The water cooled condenser is made of 11 mm o.d. glass tubing of 10 cm length.

In Table VI some combustion characteristics of various flames of interest are given. The spectral temperatures of the nitrous oxide-hydrogen flames as measured here are presented in Table VII. No Abel corrections are applied (Avni and Klein (1973)).

In a comparison of the flame temperatures we see a difference of 200°K between the conventional premixed and miniaturized diffusion nitrous oxide-hydrogen flames. This temperature drop is less than the difference between conventional hydrogen-entrained air and conventional air-hydrogen premixed flames ($\Delta t \approx 600°K$). The effect of miniaturization has apparently not greatly decreased the flame temperature. Although some drop in temperature occurs, the miniature flame still exceeds the desired 2500°K limit. The temperature of the miniature nitrous oxide-hydrogen diffusion flame is then about midway between that of air-acetylene and nitrous oxide-hydrogen premixed systems.

The new nitrous oxide-hydrogen diffusion flame exhibits a number of important desirable characteristics needed in atomic fluorescence. The temperature is in the range where particles and salt crystals are

Table VI. Combustion Characteristics of Flames of Interest (from Kirkbright and Sargent (1974)).

Mixture	(Ox/fuel)	Temp(°K)	Burning Velocity (cm/sec)
Entrained	Air/H_2	1577	---
Premixed	Air/H_2	2318	310
Premixed	N_2O/H_2	2880	390
Premixed	Air/C_2H_2	2500	150
Premixed	N_2O/C_2H_2	2990	160

Table VII. Temperature of N_2O/H_2 Flames (present work).

Mixture	Ox/fuel	Temp°K	σ(°K)
Conventional pre-mixed	N_2O/H_2	2820	21
Miniature diffusion	N_2O/H_2	2630	76

readily vaporized and diatomic species readily dissociated. A very important point to note is that in this flame the effect of burning velocity has been eliminated. Miniaturization is possible and an electrothermal atomizer may be placed inside the burner head without danger of oxidation or detonation. The burner port opening does not have to be extremely small because there is no flashback problem with this flame even at very low flow rates. The emission background of the flame is low. While it does exhibit a fluorescent background, there is very little noise associated with the background of the nitrous oxide-hydrogen flame. It appears to be a favorable flame for atomic fluorescence spectrometry.

Chapter 3

Electrothermal Atomization

Introduction

The use of flame atomization in atomic fluorescence has followed closely its use in atomic absorption. On the other hand, the use of electrothermal atomization has played a relatively minor role in atomic fluorescence work as compared to its use in atomic absorption.

King (1908) first used an electrothermal atomizer for emission studies. In 1956 Mandelshtan, Semenov and Turovtseva (1956) used a graphite cup electrothermal atomizer to deposit sample on a graphite electrode for D.C. emission spectroscopy. In 1959, L'vov (1959) began publishing his work on the applications of electrothermal atomization for atomic absorption spectrometry. Massmann (1967) produced the first electrothermal atomizer that could be used in a routine analytical laboratory. Then Massmann (1969) adapted it for use in atomic fluorescence. Development of the electrothermal atomizer for atomic absorption continued with a carbon filament (West and Williams (1969)), metal filament atomizer (Bratzel, Dagnall and Winefordner (1969)), a tantalum boat atomizer (Donega and Burges (1970)), graphite rod (West and Williams (1969)), graphite cup (Varian Techtron), and flexible graphite braid filament (Montaser, Goode, and Crouch (1974)).

A review by Dresser, Mooney, Heithmar, and Plankey (1975) covers the development and present use of electrothermal atomizers. Fuller (1974 and 1976) presented a kinetic theory of atomization and inter-

ferences encountered in electrothermal atomic absorption. Sturgeon, Chakrabarti, and Langford (1976) showed that a combined thermodynamic-kinetic model was needed to describe electrothermal atomization. Sturgeon (1977) also reported factors affecting atomization in electrothermal atomic absorption. This sample loss mechanism in electrothermal atomization has been determined to follow a simple diffusion law in some cases. In other cases considerable deviation was noted (Woodriff, Marinkovic, Howald, and Eliezer (1977)). The major loss in a Massmann furnace appears to be diffusion to cooler regions where condensation occurs. Loss through the sample ports amounted to 20% and sample loss through the porous graphite furnace walls, was ∿20% (Sturgeon and Chakrabarti (1977A)). Coating the atomizer with pyrolytic graphite has been shown to increase the signal and the life of graphite atomizers (Culver (1975)). The temperature of the gas phase analyte in the atomizer has been shown to be as much as 1300°K lower than the furnace wall temperature (Sturgeon and Chakrabarti (1977B)). This could account for numerous condensed phase and spectral interferences that are prevalent in graphite furnace determinations.

Electrothermal Atomization in Atomic Fluorescence

An electrothermal atomizer would seem an ideal atomization cell for atomic fluorescence. In reality it leads to severe condensed phase, "smoke" induced light scattering, and other interferences. The problem is much worse with continuum excitation than with "line" sources. In an effort to overcome these problems in atomic fluorescence, a technique incorporating a high temperature flame

(few interferences, low atom concentration) with an electrothermal atomizer (high atom concentration, severe spectral interferences) has been developed. Chuang and Winefordner (1975) have used a graphite filament for continuum excited atomic fluorescence.

Montaser, Goode, and Crouch (1974) used a graphite braid for determination of Cd and Zn using a line source. Detection limits were reported at approximately 5 ng/mL in both cases. Serious problems arise with electrothermal atomizers due to matrix interferences. Alger, Anderson, Maines and West (1971) have investigated problems associated with the sample matrix (other than light scattering). They have found that as the viewing height above the atomizer is increased, the apparent analyte atom population decreases exponentially. In the presence of complex matrices the apparent atom population decreases at an even faster rate. Just above the surface the apparent analyte atom population is not affected. Winefordner (1978) has suggested that it is impractical to make analytical observations near the surface of furnace walls due to high levels of blackbody radiation which lead to excessive noise levels. Therefore the viewing region must be well above the atomizer surface, resulting in a loss of sensitivity.

Preliminary Atomic Fluorescence Studies: Conventional Atomizers

In the present studies, continuum excited atomic fluorescence measurements were carried out with a graphite cup (figure 12) and also a tantalum strip atomizer. Modifications were made on the tantalum strip of Everson (1973) and Schrenk (1978) to adapt it for atomic fluorescence by addition of a port for 90° excitation.

Figure 12. Electro-Thermal Atomizer using an EIMAC continuum source.

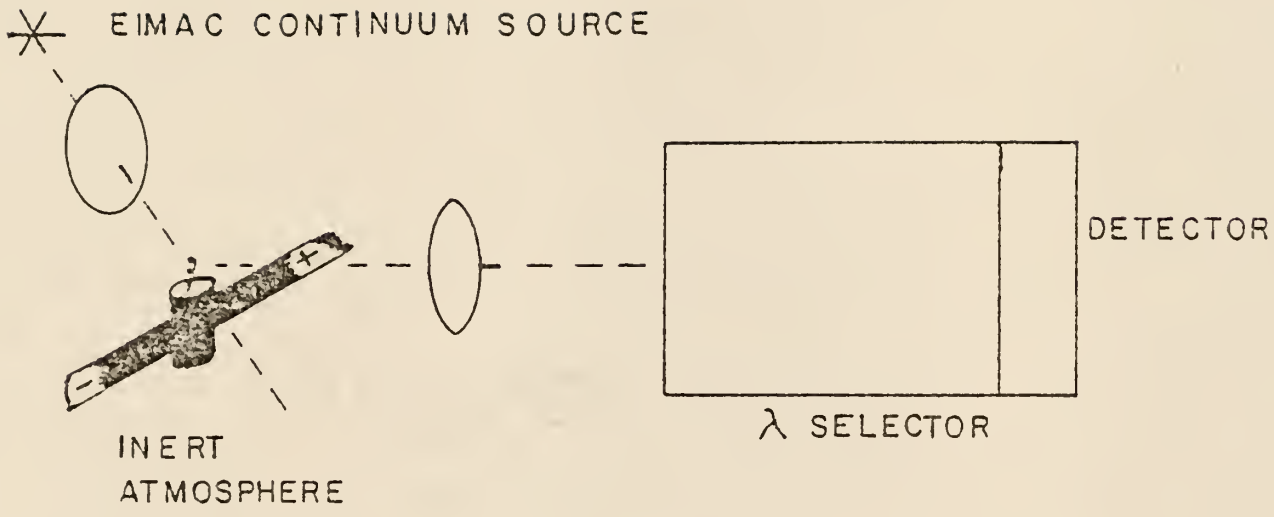
EIMAC CONTINUUM SOURCE
DETECTOR
λ SELECTOR
INERT
ATMOSPHERE

In the open design of figure 12, neither atomizer was successful in the present continuum excited atomic fluorescence studies. An excessive light scattering signal interference was encountered that obscured any atomic fluorescence that may have occurred. The background emission of the atomizer was spatially masked at the entrance slit of the monochromator, but the scattering interference was still overwhelming. This interference occurs because many particles enter the relatively cool viewing area without being completely vaporized. Sturgeon and Chakrabarti (1977B) showed in graphite furnace atomic absorption that the temperature reached by the analyte species in the gas phase is controlled by a combination of analyte volatility, the temperature attained by the furnace wall surface, and the heat transfer properties of the sheathing gas. Bystroff, Layman, and Hieftje (1979) indicated that sample particles may be introduced into the viewing region since the sample is heated in layers from the bottom up; the top layers of dried sample may be disrupted by the boiling lower layers thereby spattering particles into the viewing cell. Smoke particles from the furnace itself may also be present. The ability to vaporize these particles then depends on the gas temperature above the furnace surface. The difference (Δt) between gaseous analyte temperature and furnace wall temperature in the worst case was found to be 1300°K for indium (Sturgeon and Chakrabarti (1977B)). Another problem associated with lowered gas temperatures is that atomic species may condense or recombine after leaving the surface of the furnace. The Δt measurements were made in an enclosed furnace. In a cup design such as that of figure 12 the Δt value

between furnace wall and gas temperature may be even larger. This may aggravate the condensation loss and increase the scattered light signal markedly. An additional problem that may arise is molecular fluorescence of undissociated gaseous NaCl, $CaCl_2$, etc. from the sample matrix.

Internalized Atomizer Development

To overcome these severe and limiting interferences, a means to incorporate an electrothermal atomizer and a miniature flame was developed* (see figure 13) to maintain high atom concentrations and reduce interferences with a high temperature flame. It consists of two basic platforms. The top is stationary to allow a "fixed" viewing region. The lower assembly rotates, so that a new sample may easily be externally pipetted into the graphite cup atomizer. The assembly is then rotated back into its original position under the burner head. A programmed current sequence is then applied to dry, ash, and atomize the sample. The low flow rate stream of hydrogen carries the vapor cloud into the flame.

A more detailed drawing (figure 14) shows the atomizer and burner sections. B_2 is electrically isolated by teflon gaskets from the rest of the device. The positive and negative sides of B_2 are further separated from each other by additional teflon gaskets (dotted line in center). A sliding seal allows all of section B to rotate while maintaining a gas tight seal with section A. Hydrogen gas flows

---

* See Appendix A for construction specifications.

Figure 13. Miniature Diffusion Flame and Graphite Cup Atomizer

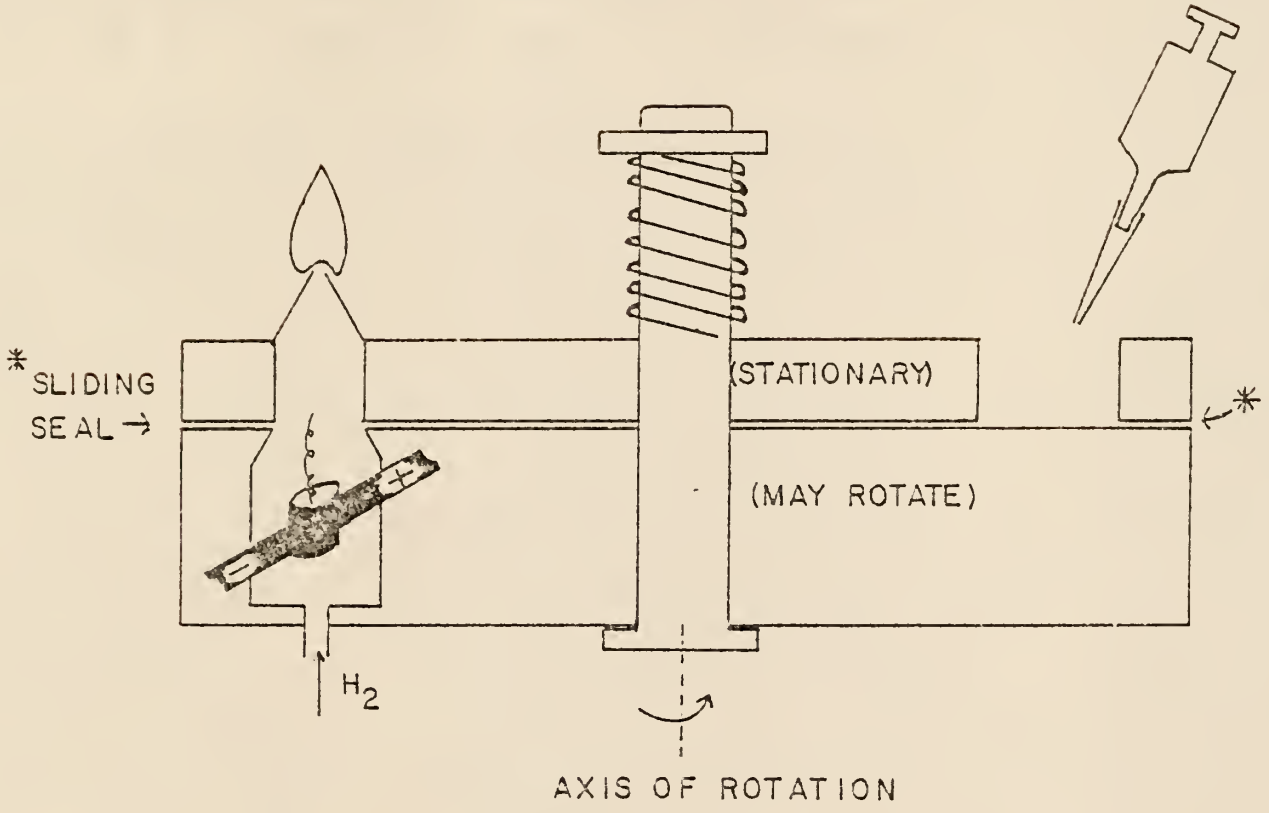
*SLIDING SEAL →
(STATIONARY)
(MAY ROTATE)
←*
H2
AXIS OF ROTATION

Figure 14. Miniature Diffusion Flame and Graphite Cup Atomizer; Showing the Graphite Cup and Burner Arrangement.

A. stationary platform

B_1. top of rotating platform

B_2. section containing atomizer

B_3. bottom of rotating platform; carrier gas introduced below cup.

Dotted line indicates a Teflon gasket to isolate + and - contacts.

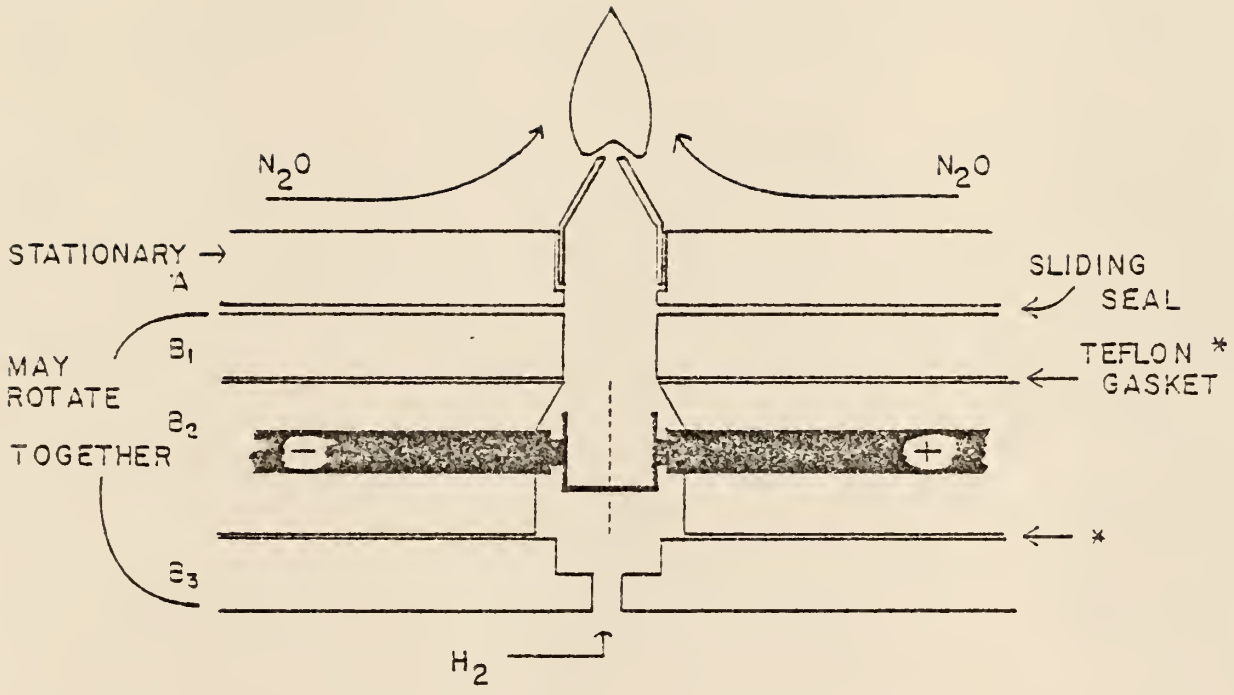
N_2O
N_2O
STATIONARY → A
SLIDING SEAL
MAY ROTATE
B_1
TEFLON * GASKET
B_2
TOGETHER
−
+
*
B_3
H_2

through B_3 around the cup and sweeps the atom cloud into the nitrous oxide-hydrogen flame above section A. Nitrous oxide surrounds the external portions of the burner head above section A to form a laminar flame as it diffuses into the hydrogen stream emerging from the burner head.

Figure 15 is a top exploded view of individual sections A, B_1, B_2, and B_3. In section A, (a) is the sample introduction post, (b_1) is a hole for the connecting bolt, (c_1) is the burner head. In section B_1, (b_2) is the same as b_1 (bolt hole), c_2 is the passage from the atomizer to the burner. In section B_2, (d) is a spacer, (e) is the atomization cell enclosure and electrode holders showing water cooling and flexible power cables attached (g) and (h) are Teflon gaskets. (i) is the opening where the graphite cup is placed. In section B_3, (b_3) is the same as b_1 (bolt hole), (c_3) is the port where the hydrogen gas enters.

The overall system is as previously described (see figure 1). The miniature flame electrothermal atomizer replaced the conventional flame (figure 1, part E). All operational parameters and instrument settings remained the same (see Table II and III) except as noted. Power for the device was obtained from the power supply of a Varian Techtron model 61 Carbon Rod Atomizer. Atomization surface temperatures were measured by thermocouple and optical pyrometry (see Appendix B) and were optimized for each element. Table VIII shows experimental operating conditions for the atomizer. Flame conditions and observation heights were optimized for cadmium. These conditions were then used throughout the study. No attempts were made

Figure 15. Miniature Diffusion Flame and Graphite Cup Atomizer;

Top Exploded View.

A. Stationary section

a = sample introduction port

b_1 = hole for connecting bolt

c_1 = burner insert

B_1. Top rotating section

$b_2 = b_1$

c_2 = passage from atomizer to burner

B_2. Atomizer cell section

d = spacer

e = two piece atomizer cell showing water cooling and flexible power cables.

f = power buss

g = Teflon gaskets separation "+" and "-" sides

h = g

i = opening where graphite cup is placed

B_3. End plate

$b_3 = b_1$

c_3 = port for hydrogen gas introduction into atomizer cell

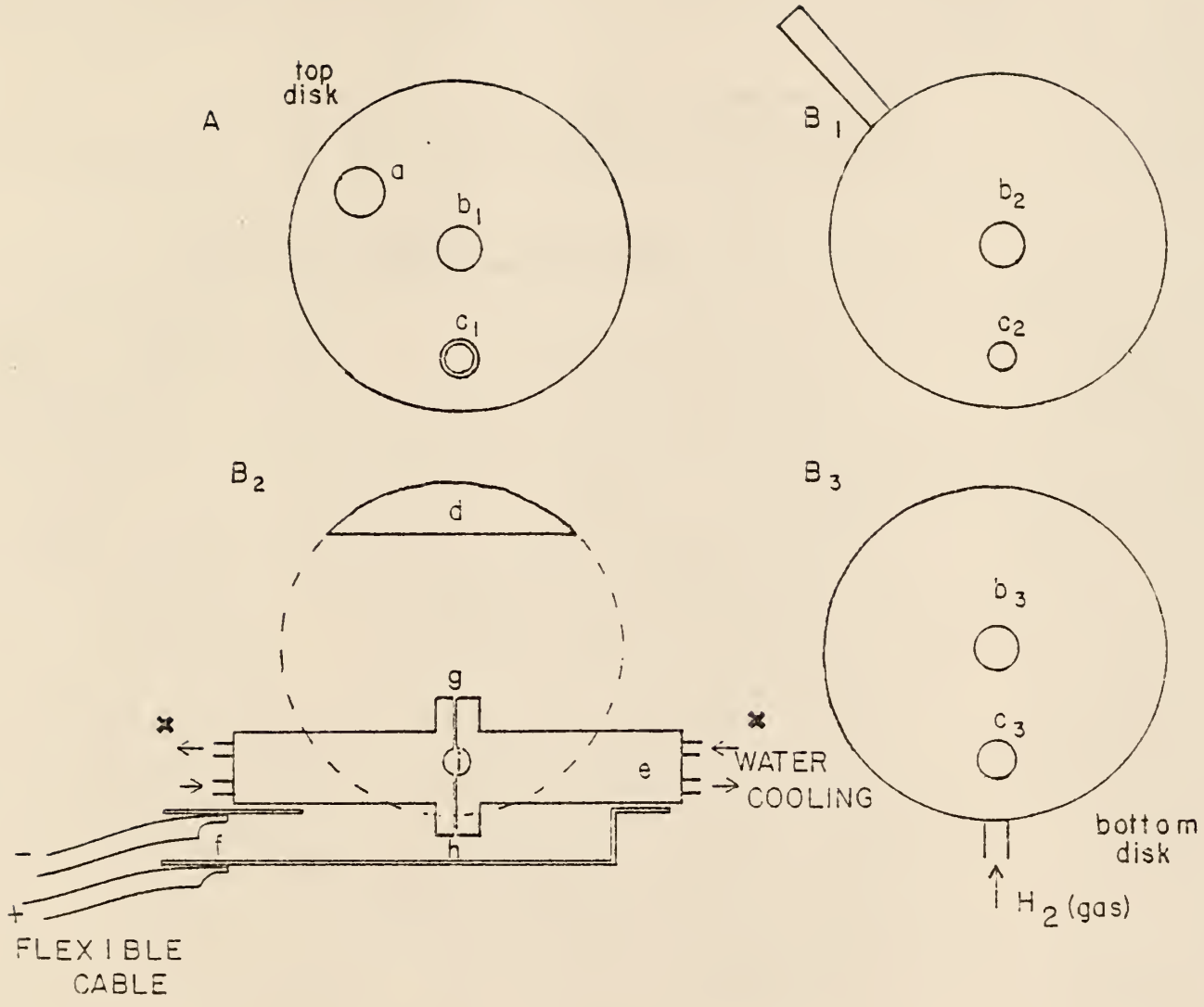
A
top
disk
a
b1
c1
B1
b2
c2
B2
d
g
e
f
h
WATER
COOLING
FLEXIBLE
CABLE
B3
b3
c3
bottom
disk
H2 (gas)

Table VIII, Experimental Conditions for Atomization Studies.

element	wavelength (nm)	Atomizer Temperatures (°K) dry	ash	atomizer
Cd	228.8	120	400	2500
Cu	324.7	120	400	>2850
Mn	279.5	120	400	>2850

Time Constant - 100 msec

Sample size - 20 µl

Cooling water - 10 ml/min

element	Atomizer Time (sec) dry	ash	atomizer
Cd	20	30	4
Cu	20	30	4
Mn	20	30	4

to further optimize the monochromator slit width, flame conditions or observation heights in the flame for other elements. The slit width was chosen as the narrowest allowable for a future computer controlled, rapid sequential, slew-scan multi-elemental analysis system (now in the planning stage). Stock solutions were made from reagent grade chemicals. Standards were prepared according to Smith and Parsons (1973).

Burner Head Design and Evaluation

For further evaluation of the diffusion flame, four burner heads were constructed (see figure 16). The signal differences among the three single hole burners were small. The signal from the seven hole burner was only one third that of any single hole burner. This is possibly due to the failure of this burner to confine the sample to an area within the 3mm diameter EIMAC lamp image. Atomic absorption measurements then indicated less difference between the seven hole and the single hole burners when the viewing area is less confined.

Enhancement of Atom Concentration in Flames

The miniature flame-internal graphite cup combination proved successful for continuum excited atomic fluorescence as indicated by Table X. The overall signal produced by the miniature flame and electrothermal atomizer was 30 times greater than that of a conventional premixed air-acetylene flame when compared on a concentration basis. When compared on an absolute (weight) basis, a signal improvement of ∿140 times is evident. This clearly indicates that

Figure 16. Burner Design for Miniature Flames

A. seven hole burner

B. one of three single hole burners

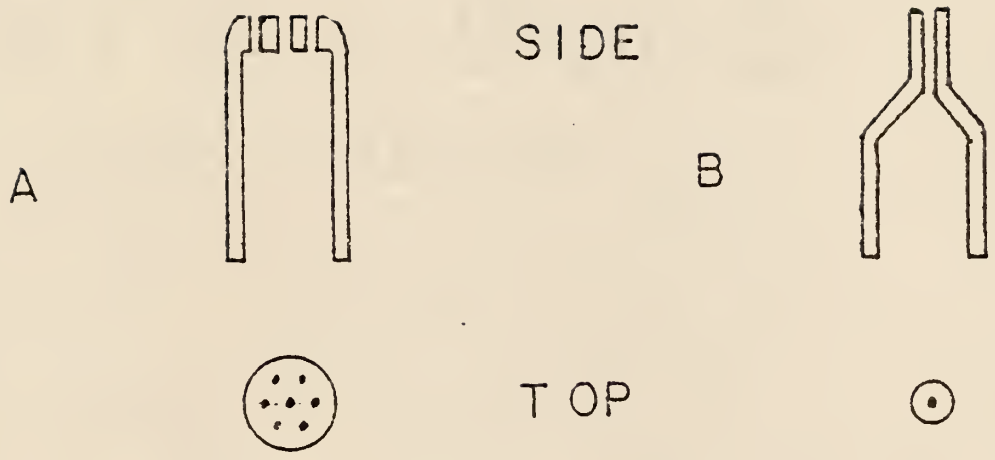
A
SIDE
B
TOP

Table IX. Detection Limit

Element	Detection Limit* (µg/ml) [a]MFIEA (TC=100ms)	[b]FAF (TC=100ms)	FAF (TC=10 sec)
Cd	.011	.5	.06
Cu	.013	-	-
Mn	.020	-	-

*as defined by Ramirez-Munoz (1968).

Table XI. Raw Signal

Element	Signal Intensity [a]MFIEA	[b]FAF
Cd	186	6

a) MFIEA - miniature flame internalized electro-thermal atomizer

b) FAF - Flame atomic flourescence

c) TC - time constant

miniaturization has in fact yielded the expected increase in atom concentration. When both signal and noise are taken into account, the improvement in continuum atomic fluorescence detection limit of the miniature flame is ∿50 fold on a concentration basis and ∿230 fold on a weight basis. These comparisons are made of equivalent read out time constants of 100 msec. Since the conventional premixed system is inherently a steady state system and the miniature system produces transient signals, it must be conceded that longer time constants will lower the detection limit of the premixed system by averaging the effects of noise (if sufficient sample is available). The miniature system, on the other hand, favors the 100 msec time constant condition. The overall comparison is then a ∿5 fold improvement in concentration detection limit and ∿27 fold improvement in absolute detection limit for the new approach when unlimited sample is available. If microsampling is required due to limited sample volume ($\leq$ 0.2 ml), then a 100 ms time constant must be used in all cases and a ∿50 fold improvement in concentration detection limit and a ∿230 fold improvement of weight detection limit is realized with the new atomic fluorescence method. In atomic absorption, there was a signal improvement of 5 to 8 times over flame (see Table XI in Spectral Continuum Interference section) on a concentration basis and ∿28 times on a weight basis.

These studies have indicated that despite any time constant-noise considerations, the raw signal indicative of atom concentration is enhanced by miniaturization. Further sensitivity improvement should be the goal of future studies. The author believes that this

would best be accomplished by further reduction of internal dimensions and gas flow rates. This would reduce the amount of diffusion that occurs before the sample reaches the viewing cell.

Precision

The precision of this method is generally limited by the reproducibility of the atom concentration in the viewing region. The contribution to variance by other electronic and optical factors is generally small with respect to the atomizer contribution. The reproducibility of this atom concentration is influenced by the following factors: the reproducibility of the pipetting technique, the placement of the sample in the cup, the stability of the gas flow rate, and the heating rate of the cups as affected by the condition of the graphite electrode contacts. These effects are all similar to the situation in graphite furnace atomic absorption. In the present combined miniature flame, electrothermal atomizer for atomic fluorescence, one other factor affected the reproducibility. This was solvent vapor that condensed in the cooler passageways and inside the burner head during the dry cycle. On initiation of the atomization cycle the additional heating of the chamber area caused the condensed water to boil vigorously, which significantly degrades the precision of the overall result.

To overcome this problem, the cooling water circulation rate was reduced so that the atomizer cell and passageways remained hot enough to prevent solvent condensation during the dry cycle. This was accomplished at a flow rate of 10 mL/min of cooling tap water. If the atomizer cell's temperature was allowed to rise higher yet,

the reproducibility again suffered. The final percent relative standard deviation on a day to day basis was determined to be less than or equal to 5% at concentrations greater than or equal to 10 times the detection limit.

Transport Phenomena

One of the problems of an internal atomizer is the sample loss. Woodriff, Marenkovic, Howald, and Eilizer (1977), and Sturgeon and Chakrabarti (1977A) determined that the major sample loss mechanism in a graphite furnace is diffusion to cooler furnace extremities and condensation there.

Previous workers have used electrothermal atomizers for sample introduction in flame emission (Grime and Vickers (1976)) and in plasma emission (Runnels and Gibson (1967), Fricke, Rose, and Caruso (1975). Gibson Nixon, Fassel, and Knoseley (1974), and Gunn, Millard, and Kirkbright (1978)). The systems were not miniaturized and did not involve diffusion flames or atomic fluorescence. Only Gunn, Millard, and Kirkbright (1978) investigated sample transport in an enclosed electrothermal atomizer system for atomic emission. The internal chamber volume was approximately one liter. The sample was required to travel a minimum of 0.5 meters to reach the plasma. When the traveled path leading to the plasma was increased to 20.5 meters, the signal peak broadened in time, but little change was noted in the time integrated response. It was assumed therefore, that analyte was not condensing (or at least not adhering to the tube walls leading to the plasma). Kirkbright acknowledged that some of the analyte is undoubtedly lost initially as the vaporized material rapidly

cools and condenses in the chamber immediately surrounding the electrothermal atomizer. If the sample cools sufficiently to crystallize or condense while suspended in the flowing gas, it may not adhere to any wall surfaces but rattle on through to the plasma or flame instead. The condensate problem was studied for cadmium samples. Glass simulated burners were constructed (see figure 17), one to approximate the miniature metal burner, one that was 40 cm in height, and one to approximate the passageway from the atomizer cell to the flame plus the burner (all in glass). Two micrograms of cadmium were pipetted into the graphite cup (situated below the "all glass" simulated system). No flame was burning, but the system was otherwise operated under the same conditions as described earlier (Table VIII) Deionized water blanks were measured under similar conditions. "Burners" A and B were then soaked in 0.1N nitric acid for three minutes. "Burner" C was sealed with Parafilm, filled with 1 ml of 0.1N nitric acid and capped with Parafilm. All glass and Parafilm used were cleaned in concentrated nitric acid and rinsed with deionized water. Care was taken in handling glass burners A and B to avoid contamination of the outsides. All tests were taken in replicates of three. After atomizing samples and blanks in the graphite cup, each glass burner was rinsed in acid as described above. The rinsings were then assayed for Cd by graphite furnace atomic absorption (PE 603). The rinse assay indicated that about 1% of the sample was found to condense in "burner" A. 3% was found to condense in "burner" B. In "burner" C ~24% of the sample condensed on the walls (see Table X). These measurements indicate that the major part of the loss was accounted

Figure 17. Simulated Glass Burners for Condensate Studies

A. Simulated Glass Burner Head

1.2 cm tall by 0.7 cm wide

B. Simulated Glass Burner Head

40 cm tall by 0.7 cm wide

C. Simulated Glass Burner Head and Passageway

3.0 cm tall by 0.7 cm wide

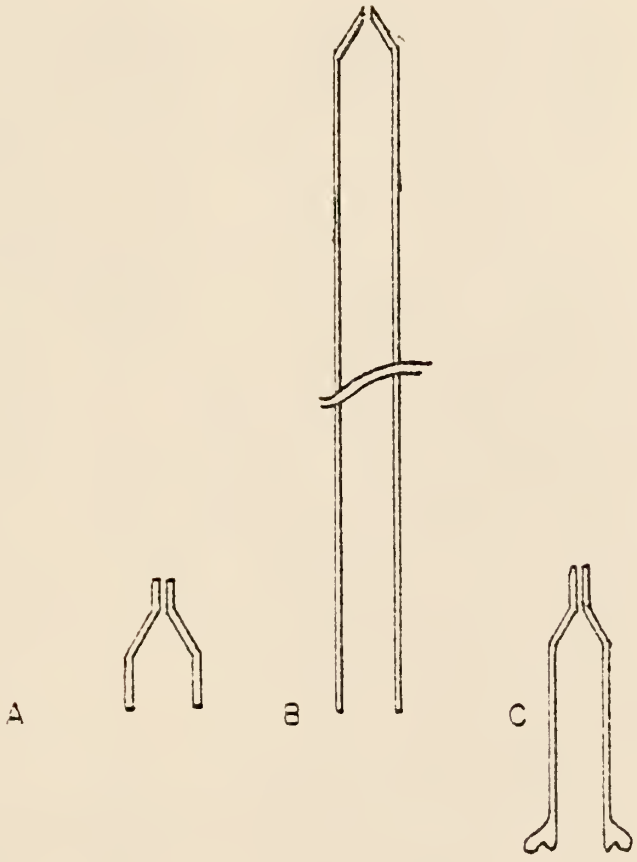
A
B
C

Table X, Condensate Magnitudes

simulated burner	Cd present (ng)	% of total
A	22	1,1
B	51	2.6
C	470	23.5

for in the first few centimeters of the passageway leading from atomizer to burner. The sample loss appears to be only a total of ∿24% for Cd. It is possible that elements with lower vapor pressures may suffer greater condensation losses. Several of these are currently under study in this laboratory.

Spectral Continuum Interferences

One of the most important parameters studied in this research project was that of the line-to-background ratio where spectral interferences are concerned. For example, our technique of electrothermal atomizer-continuum excited atomic fluorescence was not successful until the flame was added to vaporize particles etc. that otherwise yielded severe interference signals. It is then further relevant to study the additional background caused by high concentrations of sample matrix salts. Line to background ratios were first determined by atomic absorption with the cadmium atomic resonance line at 228.8 nm and the "nonabsorbing" Cd ion line emitted by the hollow cathode discharge at 226.5 nm. 10% NaCl was used to measure the background due to matrix salts. The NaCl background in the AA mode is the molecular absorption of diatomic gaseous NaCl.

Atomic fluorescence line and background measurements were then made with the cadmium 228.8 nm line and then stepping off the analytical wavelength to 228.0 nm to measure the background from a 10% NaCl solution. No attempt was made to determine whether the NaCl background measured in the atomic fluorescence mode was due to light scattering or to the fluorescence of NaCl. Hollow cathode atomic absorption results of the present research are given in Table XI

Table XI. Line: Background Ratios[a]

Atomizer	Path, cm	Cd Line (L) Atomic Absorbance /ppm	NaCl Background (B) Abs./% NaCl	(L/B) Ratio
Premixed N_2O-C_2H_2	5	0.06	0.00042	143.0
Electrothermal[b] Miniature Flame (N_2O-H_2)	<.5	1.67 (0.167 A, 0.1 ppm Cd, 20 µL)	.0137 (0.137 A, 10% NaCl, 20 µL)	121.8
Premixed Air-C_2H_2	10	0.30	0.0035	84.7
Carbon Rod Analyzer	1	147.	6.0	24.4
Total consumption system	40	3.5	0.6	5.8

a) all values from Fry and Denton (1979) except b

b) from present studies

along with earlier values from Fry and Denton (1979), for conventional flame and carbon rod atomizer.

In an atomic absorption mode the line to background ratio of the miniature diffusion flame is shown by Table XI to be between that of premixed air-acetylene and nitrous oxide-acetylene flames. This is approximately what would be expected from temperature considerations. The ratio is better than air-acetylene, but not as good as nitrous oxide-acetylene. The important result is that the line to background ratio in atomic absorption using the miniature flame is similar to that of conventional premixed flames and significantly better than that of graphite atomizers. The analyte sensitivity is also better than that of premixed flames, although not as good as open furnaces. Further developments are needed to improve the atomic absorption sensitivity of the new system while still maintaining the favorable line to background ratio inherent in premixed flames. Investigations of signal, noise, and background as a function of slit width in continuum excited atomic fluorescence yielded an overall "best" signal to background and signal to noise ratio at a slit setting of 200 μm (see Table XII). At 400 μm the S/N ratio is better, but the line to background ratio is not as good. The miniature diffusion flame results of this study indicate that introduction of a 10% NaCl solution poses no major problem. This is in sharp contrast to conventional electrothermal atomization for which Culver (1975) has shown to yield severe interference when samples as dilute as 0.1% NaCl are introduced. 10% NaCl in a conventional premixed nitrous oxide-hydrogen flame also showed no response other than an increase in noise.

Table XII. Line, Background, and Noise as a Function of Slit Setting

slit setting (μm)	Noise Amplitude (N)	Background[a] (B)	Line[b] (L) (also signal(S))
50	1.0	.3	20.6
200	4,5	1,0	186.1
400	10.	13.3	520.0

slit setting (μm)	S/N	L/B
50	20.6	68.7
200	41.35	186.1
400	52.0	39.3

a) 10% NaCl, 20 μl sample, signal normalized to 1% NaCl.

b) 0.5 ppm Cd, 20 μl sample, signal normalized to 1 ppm Cd.

Chapter 4

Summary and Conclusions

The miniature nitrous oxide-hydrogen laminar diffusion flame developed in this work has a number of characteristics that make it useful for atomic fluorescence spectrometry. There is no tendency for flame flashback; large burner port openings may be used if desired. The flame provides high temperature with low background emission, low noise, and is very good at vaporizing particles and dissociating compounds. These properties result in reduced interferences from complex sample matrices and may allow reliable analysis of many sample types of relatively high salt content.

With the electrothermal atomizer, the atom concentration in the miniature flame was significantly higher than with conventional flame systems. The design allows for easy sample introduction and operation. Required sample volumes are small (20 µl). The reproducibility of the system allows for minimal sample trial replication. The miniature flame allows the electrothermal atomizer to be operated at temperatures approaching the sublimation temperature of carbon with minimal interference effects. This would not be possible with a graphite atomizer operated in the conventional mode. Although the life of the cup is reduced, atomizing at elevated temperature may allow determination of more refractory elements.

Condensation losses appear to be only about 25% for cadmium. The losses occur on the wall surfaces in close proximity to the graphite atomizer.

Background due to light scattering and molecular fluorescence by sample matrix species and furnace smoke represents the most severe problem encountered in electrothermal atomizer atomic fluorescence with a continuum excitation source. For analysis of complex samples, the line to background ratio is even more important than the signal to noise ratio in continuum atomic fluorescence. Atomic fluorescence determinations with the tantalum strip and with an open carbon cup had a line to background ratio of approximately zero. Even if the signal to noise ratio had been excellent, no useful information would be obtainable from such a system.

The new miniature diffusion flame eliminates the severe background interference otherwise encountered with electrothermal atomization in continuum excited atomic fluorescence. Salt concentrations as high as 10% NaCl (w/v) can be tolerated.

Chapter 5

Recommendations for Future Studies

The investigation of "hotter" diffusion flame mixtures (atomic hydrogen, $O_2/(CN)_2$, Cl_2/H_2 and F_2/H_2) may prove useful (especially for flame emission). Improvement in the graphite cup design might play an important role in sample introduction and in lowering the detection limits. A further reduction in size of the burner head may improve the detection limits by decreasing the effects of diffusion. Sample loss via condensation should be investigated for other elements. A heated graphite burner head may alleviate this problem and aid in the design of a further reduction in system size. The development of a multiple internal atomizer arrangement on a rotating turret, auto sampler, and slew-scan monochromator under computer control is suggested for multi-elemental analysis. Parallel drying and ashing cycles followed by rapid sequential atomization cycles of the multiple furnaces could increase analysis rates to twenty determinations per minute. Further line to background ratios should be measured for samples such as whole blood, etc. A slightly longer path burner with small internal dimensions should be designed for atomic absorption.

Appendix A

Construction Details of the Electrothermal Atomization Cell

Figure 18 shows a cross section and figure 19 shows a top exploded view of the electrothermal atomization cell. In both figures A, B_1, B_2, and B_3 are the same. A, B_1, and B_3 are nickel plated brass disks 3 inches in diameter by 3/8 inches thick. B_2 is the graphite cup section. It is another nickel plated brass piece (3/4 inches thick, 3/4 inches wide, and 4 inches long). It is made in two pieces so that each side is electrically isolated (by Teflon) from the other. B_1 and B_3 are also electrically isolated from B_2 (again with Teflon).

In figure 18, C is the burner head described in the section on burner head design. D is the passage way from the atomizer to the burner head (1/4 inches in diamter). E is a spectral grade graphite rod (1 1/4 inches long by 1/4 inches in diameter). It has been undercut to a diameter of 0.19 inches over a length of 0.19 inches at the graphite cup contact. The contact area has been plunge milled using a 0.25 inch end mill to the contour of the graphite cup (for proper electrical connection). G is a PT-101 Graphite Electrode (crater only, pyrolytically coated) from Ultra Carbon (0.25 in o.d., 0.19 in. deep, 50 µl crater volume). F is a chamber surrounding the graphite cup. The bottom opening is 11/16 inches and the top 1/4 inches in diameter. It starts tapering just above the electrodes. The total internal volume (from B_2 to the tip of the burner head) is 1.5 ml.

In the top exploded view (figure 19) (a) is 1/2 inches in

Figure 18. Construction Diagram; Side View

A. stationary platform

B_1. top of rotating platform

B_2. section containing atomizer

B_3. bottom of rotating platform carrier gas introduced below cup

C. burner head

D. passageway

E. graphite electrode

F. internal chamber

G. graphite cup

The dotted line indicates a Teflon gasket to isolate + and - contacts on cup.

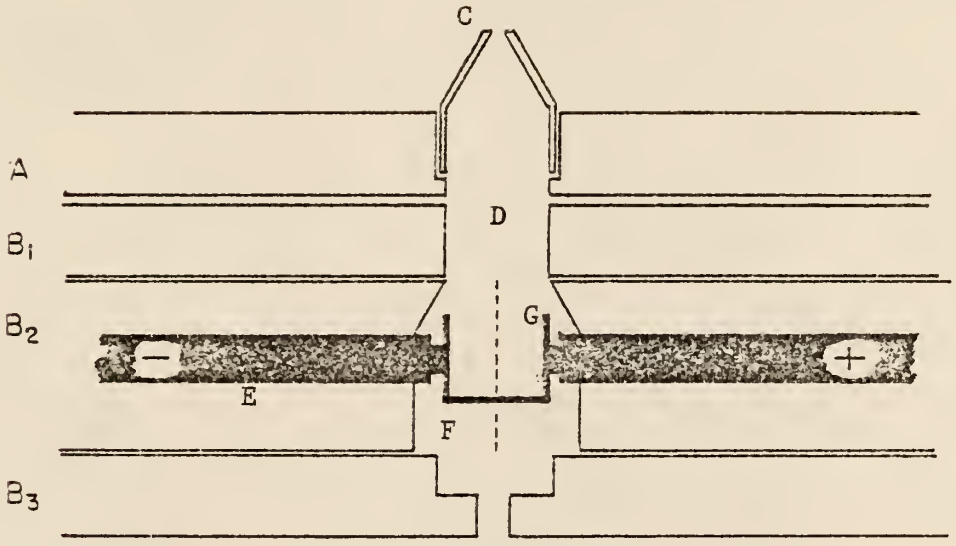
C
A
D
B1
B2
G
E
F
B3

Figure 19. Construction Diagram; Top Exploded View

A. Stationary section

a = sample introduction port

b_1 = hole for connecting bolt

c_1 = burner insert

B. Top rotating section

$b_2 = b_1$

c_2 = passage from atomizer to burner

B_1. Atomizer cell section

d = spacer

e = two piece atomizer cell showing water cooling and flexible power cables. "+" and "-" sides separated by teflon gaskets.

B_3. End plate

$b_3 = b_1$

c_3 = port for hydrogen gas introduction into atomizer cell

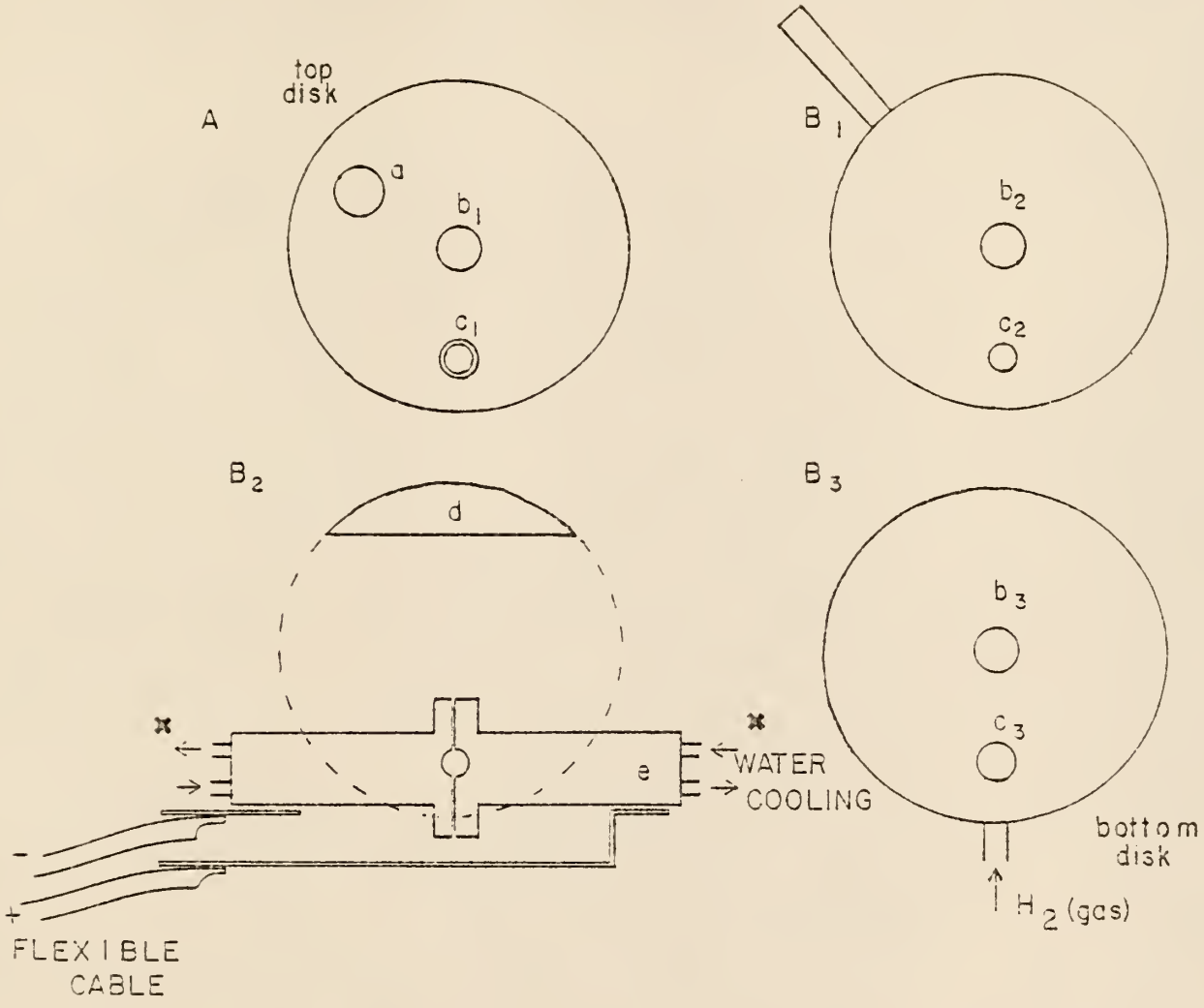
top
disk
A
a
b1
c1
B1
b2
c2
B2
d
e
WATER
COOLING
B3
b3
c3
bottom
disk
H2 (gas)
FLEXIBLE
CABLE

diameter. b_1, b_2 and b_3 are 3/8 inches in diameter (a 3/8 inch bolt with spring tension is used to hold A and B_1, and B_2 and B_3 together). In C_1, the passageway is 1/4 inch in diameter at the common bottom then it is "stepped out" to 5/16 inch diameter at the top for the burner head. (C_2) is passageway D (figure 18). (d) is a nickel plated brass spacer (3/4 inches thick), (e) is the atomization section. It contains the graphite rods and cup. Tension on the cup is applied by two set screws with polished flat ends that press against the ends of each graphite rod. Passageways were drilled for cooling water in both sides (+ and -) of the section (the water passages are not interconnected). Power is applied to each side through a flexible power cable. (C_3) is 1/2 inches in diameter. It is used for H_2(gas) flow and access to the graphite cup.

Appendix B

Temperature Settings

Figure 20 and 21 show the dial setting vs temperature graphs of the graphite cup. The dry and ash cup temperature measurements were taken with a thermocouple. The atomization cup temprature was measured with an optical pyrometer. The dry, ash, and atomize temperature are represented by 0, X and A respectively.

Figure 20. Dial Setting vs Cup Temperature for Dry and Ash Cycles.

Dry cycle (O), ash cycle (X).

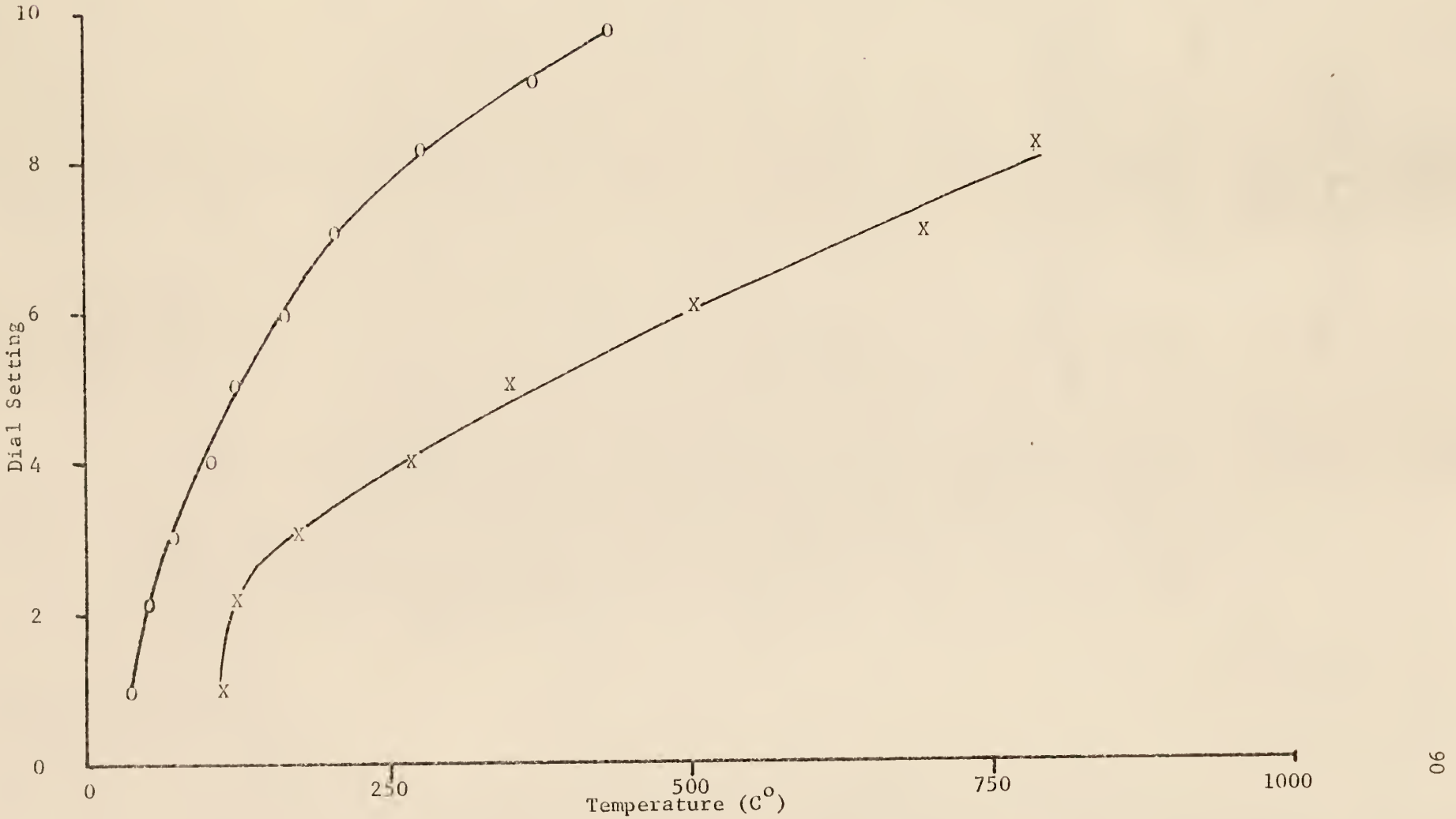
10
8
6
4
2
0
Dial Setting
0
250
500
750
1000
Temperature (C°)

Figure 21. Dial Setting vs Cup Temperature for Atomizer Cycle (A).

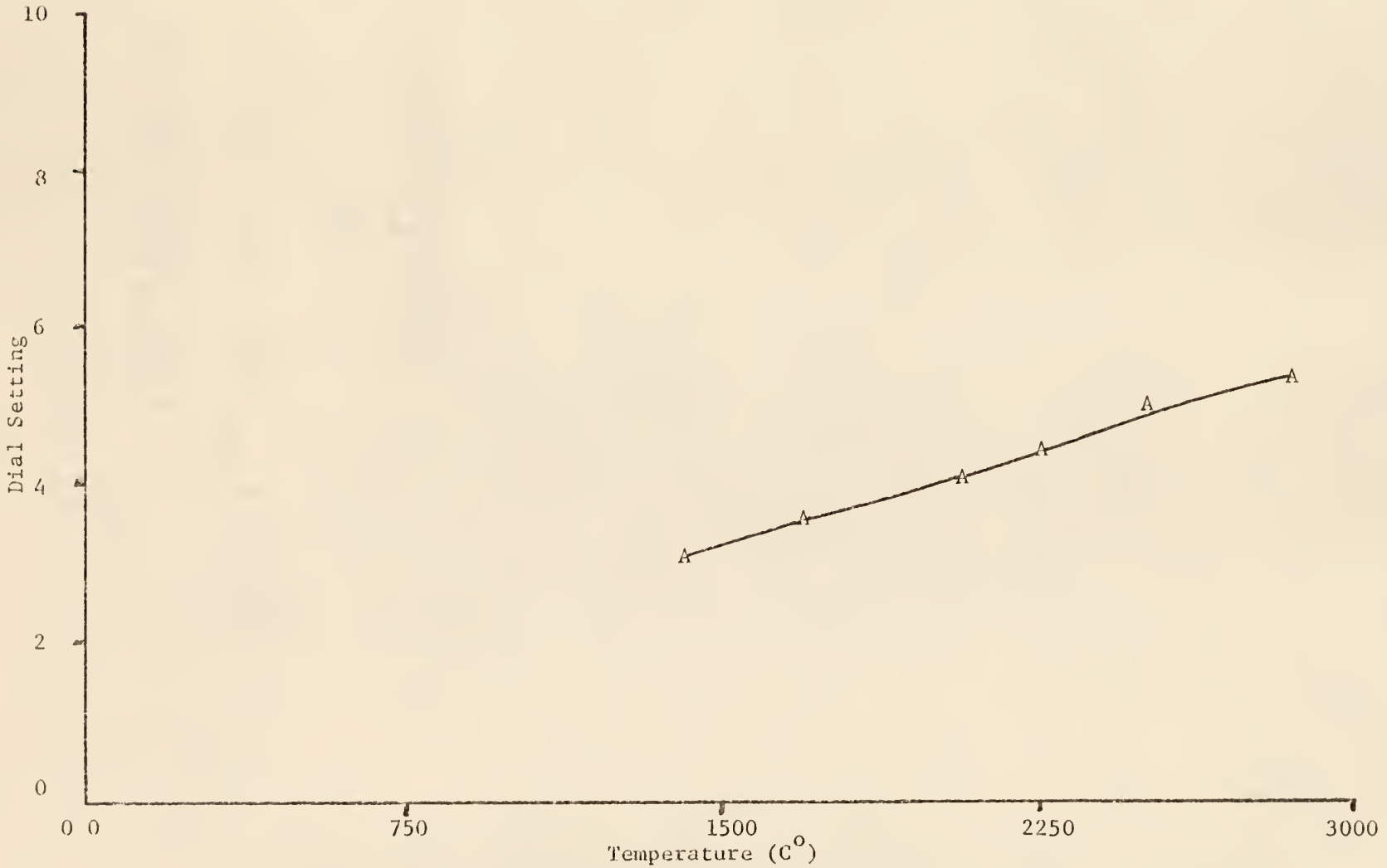
10
8
6
4
2
0
Dial Setting
0 0
750
1500
2250
3000
Temperature (C°)
A
A
A
A
A
A

List of References

Alger, D., Anderson, R. G., Maines, I. S., and West, T. S., Anal. Chim. Acta 57, 271 (1971).

Avni, R. and Klein, F. S., Spectrochim. Acta 28B, 319 (1973)

Badger, R. M., Z. Physik 55, 56 (1929).

Bratzel, M. P., Dagnall, R. M., and Winefordner, J. D., Anal. Chim. Acta 48, 197 (1969).

Bystroff, R. I., Layman, L. R., and Hieftje, G. M., Appl. Spectrosc. 33, 230 (1979).

Chuang, F. S. and Winefordner, J. D., Appl. Spectrosc. 29, 412 (1975).

Culver, B. R., Analytical Methods for Carbon Rod Atomizers, Varian Techtron Pty. LTD., Springvale, Victoria, Australia (1975).

Donega, H. M., and Burgess, T. E., Anal. Chem. 42, 1521 (1970).

Dreser, R. D., Mooney, R. A., Heithmar, E. M., and Plankey, F. W., J. Chem. Ed. 52 A451 (1975).

Everson, R., Thesis, Kansas State University (1973).

Fernandez, M. A., and Bastiaans, G. J., Appl. Spectrosc. 49, 944 (1977).

Fowler, W. K. and Winefordner, J. D., Anal. Chem. 49, 944 (1977).

Fricke, F. L., Rose, O., Jr., and Caruso, J. A., Anal. Chem. 47, 2019 (1975).

Fry, R. C., and Denton, M. B., Anal. Chem., 51, 266 (1979).

Fuller, C. W., Analyst, 99, 739 (1974).

Fuller, C. W., Analyst, 101, 798 (1976).

Fuller, C. W., Electrothermal Atomization for Atomic Absorption Spectrometry, The Chemical Society, Burlington Society, London Ch 3 (1977).

Gaydon, A. G., Proc. Phys. Soc. 56, 95 (1944).

Grime, J. K. and Vickers, T. J., Anal. Chem. 47, 432 (1975).

Gunn, A. M., Millard, D. L., and Kirkbright, G. F., Analyst., 103, 1066 (1978).

Haraguchi, H., Smith, B., Weeks, S., Johnson, D. J., and Winefordner, J. D., Appl. Spectrosc. 31, 156 (1977).

Johnson, D. J., Plankey, F. W., and Winefordner, J. D., Anal. Chem. 46, 1898 (1974).

Johnson, D. J., Plankey, F. W., and Winefordner, J. D., Anal. Chem. 47, 1739 (1975).

King, A. S., Astrophys. J. 27, 353 (1908).

Kirchhoff, G., and Bunsen, R., Pogg. Ann., 110, 161 (1860).

Kirkbright, F. G., and Sargent, M., Atomic Absorption and Fluorescence Spectroscopy, Academic Press, London, (1974).

Kniseley, R. N., Flame Emission and Atomic Absorption Spectrometry, J. A. Dean and T. C. Rains, eds, Marcel Dekker, New York, 1969 Vol. 1.

L'vov, B. V., J. Eng. Phys., 2, 44 (1959).

Mandelshtam, S. L., Semenov, N. N., and Turovtseva, Z. M., Zhir. Analy. Khim. 11, 9 (1956).

Mann, C. K., Vickers, T. J., and Gulick, W. M., Instrumental Analysis, Harper and Row, New York, N.Y., Chap. 13 (1974).

Massmann, H., Z. Anal. Chem. 225, 203 (1967).

Massmann, H., Spectrochim. Acta, 23B, 215 (1969).

Montaser, A., Goode, S. R., and Crouch, S. R., Anal. Chem. 46, 599 (1974).

Nichols, E. L., and Howest, H. L., Phys. Rev. 23, 472 (1924).

Nixon, D. E., Fassel, V. A., and Kniseley, R. N., Anal. Chem. 46, 210 (1974).

O'Haver, T. C., Harnly, J. M., and Zander, A. T., Anal. Chem. 50, 1218 (1978).

Ramirez-Munoz, J., Atomic-Absorption Spectroscopy and Analysis by Atomic Absorption Flame Photometry, p. 227, Elsevier Publishing Company, Amsterdam (1968).

Rief, I., Fassel, V. A., and Kniseley, R. N., Spectrochim. Acta, 28B, 105 (1973).

Routh, M. W., personal communication (1979).

Runnels, J. H., and Gibson, J. H., Anal. Chem. 39, 1398 (1967).

Schrenk, W. G., personal communication (1979).

Smith, B. W., and Parsons, M. L., J. Chem. Ed. 50, 679 (1973).

Sturgeon, R. E., Anal. Chem. 49, 1255A (1977).

Sturgeon, R. E. and Chakrabarti, C. L., Anal. Chem. 49, 1100 (1977A).

Sturgeon, R. E., and Chakrabarti, C. L., Spectrochim. Acta 32B, 231 (1977B).

Sturgeon, R. E., Chakrabarti, C. L., and Langford, C. H., Anal. Chem. 48, 1972 (1976).

Veillon, C., Parsons, M. L., Mansfield, J. M., and Winefordner, J. D., Anal. Chem. 38, 204 (1964).

Weeks, S. J., Haraguchi, H., and Winefordner, J. D., Anal. Chem. 50, 360 (1978).

West, T. S., and Williams, X. K., Anal. Chim. Acta 45, 27 (1969).

Winefordner, J. D., J. Chem. Ed., 55, 72 (1978).

Winefordner, J. D., and Vickers, T. J., Anal. Chem., 36, 161 (1964).

Winefordner, J. D., and Staab, R. A., Anal. Chem., 36, 165 (1964A).

Winefordner, J. D., and Staab, R. A., Anal. Chem., 36, 1367 (1964B).

Wood, R. W., Phil. Mag., 10, 513 (1905).

Woodriff, R., Marinkovic, M., Howald, R. A., and Eliezer, I., Anal. Chem., 49, 2008 (1977).

VITA

Steven Kenneth Hughes was born on April 29, 1954 in Safford, Arizona. He was the youngest child of Elmo I. and Mildred S. Hughes.

He lived in Thatcher, Arizona, until five years old, when his family moved to Wilcox, Arizona, where he attended school grades one through four. Then the family moved to Safford, Arizona. In May, 1972 he graduated from Safford High School. Then attending Eastern Arizona College (1/72-5/74) he met and then married his wife, Louise Holyoak, on May 11, 1973. In the fall of 1974 he attended Arizona State University, graduating in May, 1977 with a B.S. in Chemistry. During this time he had two children, a girl - Jeanette (Nov. 29, 1974) and a boy - Kenneth Jeramiah (July 13, 1977). He was admitted to Kansas State University to work on a Masters Degree in Chemistry in August 1977. On May 1, 1979, his youngest son Nicholas Brandon was born.

A MINIATURE FLAME FOR ATOMIZATION IN CONTINUUM EXCITED ATOMIC FLUORESCENCE SPECTROMETRY

by

STEVEN KENNETH HUGHES

B.S., Arizona State University, 1977

AN ABSTRACT OF A MASTER'S THESIS

submitted in partial fulfillment of the

requirements for the degree

MASTER OF SCIENCE

Department of Chemistry

KANSAS STATE UNIVERSITY
Manhattan, Kansas

1979

The design and characteristics of a combined miniature N_2O/H_2 diffusion flame and graphite cup atomizer are presented for continuum excited atomic fluorescence spectrometry. Data are given concerning the spectral properties, electronic temperature, burning velocity, analytical sensitivity, precision, and susceptibility to spectral continuum interferences of the new miniature diffusion flame. A comparison of the properties of this combustion mixture is made with those of a variety of other diffusion mixtures and conventional premixed flame systems. Investigations are presented concerning the transport of analyte from the graphite cup to the vincinty of the miniature diffusion flames.